

Review

Design Strategies toward Enhancing the Performance of Organic Electrode Materials in Metal-Ion Batteries

Yong Lu,¹ Qiu Zhang,¹ Lin Li,¹ Zhiqiang Niu,¹ and Jun Chen^{1,*}

Organic electrode materials have shown great potential for metal-ion batteries because of their high theoretical capacity, flexible structure designability, and environmental friendliness. However, their electrochemical performance still needs to be further enhanced, which mainly depends on the molecular structures, electrode fabrication, electrolyte, and separators. In this review, we present the working principles and fundamental properties of different types of organic electrode materials, including conductive polymers, organosulfur compounds, organic radicals, carbonyl compounds, and other emerging materials. We then focus on the strategies toward enhancing the electrochemical performance (output voltage, capacity, cycling stability, and rate performance) of organic electrode materials in various metal-ion batteries. The key challenges of organic electrode materials for metal-ion batteries mainly contain the high solubility in electrolyte, low intrinsic electronic conductivity, large volume change, and low tap density. This review provides insights into the development of organic electrode materials with high performance for next-generation rechargeable metal-ion batteries.

INTRODUCTION

The recent boom in consumer electronics, electric vehicles, and energy storage stations has raised the demand for batteries that will not only possess excellent electrochemical performance but also be safe, inexpensive, and environmentally friendly.¹ Because of their high energy density, metal-ion batteries have attracted much attention in recent years.² However, conventional metal-ion batteries are often based on inorganic electrode materials such as transition-metal oxides and graphite, which usually show low practical capacity or depend on scarce natural resources.³ In contrast, organic electrode materials are endowed with various merits.^{4,5} For instance, they generally deliver high capacity because of the considerable number of active sites per weight. Moreover, they are composed of abundant elements (e.g., C, H, O, N, and S) and can be obtained from biomass resources or through mild synthesis processes. Furthermore, the structure of organic molecules can be designed flexibly, which contributes to easy tailoring of their electrochemical performance. In addition, unlike inorganic materials, organic materials are generally not restricted by the choice of counter-ions. It is feasible to apply the same organic molecule in various metal-ion batteries.

The history of organic electrode materials can be traced back to the 1960s, when the carbonyl compound (dichloroisocyanuric acid [DCCA]) was first used in primary lithium batteries.⁶ Unfortunately, the high solubility of small carbonyl compounds in electrolyte restricts their further development. Subsequently, many conductive

The Bigger Picture

With the increasing demand for resources and environmental issues, organic electrode materials have attracted extensive attention in recent years. However, the electrochemical performance of organic electrode materials still needs to be further improved for the construction of high-performance metal-ion batteries. This review introduces the working principles and fundamental properties of different types of organic electrode materials and highlights the strategies for improving their electrochemical performance in various metal-ion batteries. The common challenges of organic electrode materials for metal-ion batteries are the high solubility in electrolyte, low intrinsic electronic conductivity, large volume change, and low tap density. Thus, future investigations of organic electrode materials should focus on improving their intrinsic electronic conductivity and tap density by molecular engineering and enhancing their cycling stability and safety via electrolyte optimization.

polymers such as polypyrrole (PPy) were explored as the electrode materials for lithium-ion batteries (LIBs), sodium-ion batteries (SIBs), and aluminum-ion batteries (AIBs) because of their limited solubility in electrolyte.^{7,8} Nevertheless, the low doping level limits their practical capacities. Thereafter, to seek new organic electrode materials with high capacity, attention was paid to organosulfur compounds in the late 1980s.⁹ However, with the successful commercialization of LIBs (cathode: LiCoO₂; anode: graphite) in 1991, organic electrode materials were gradually ignored and there were only few works concerning this topic in the 1990s and early 2000s. It was not until 2002 that organic radicals were reported as high-voltage cathodes for LIBs.¹⁰

With the increasing demand for resources and environmental issues, organic electrode materials have been extensively investigated again in the past decade.^{1,11} On the one hand, more and more new types of organic compounds such as C=N, C≡N, N=N, and multiple carbon bonds (C=C and C≡C)-based redox materials were developed.^{12,13} On the other hand, organic electrode materials were widely explored for various metal-ion batteries, including LIBs, SIBs, potassium-ion batteries (KIBs), magnesium-ion batteries (MIBs), zinc-ion batteries (ZIBs), AIBs, and calcium-ion batteries (CIBs).¹⁴ Although there are many reviews of organic electrode materials, it is noteworthy that a comprehensive review focusing on the design strategies to improve their electrochemical performance in various metal-ion batteries is still absent.^{4,7,11–15}

In this review, we first present the working principles and fundamental properties of organic electrode materials, including conductive polymers, organosulfur compounds, organic radicals, carbonyl compounds, and other emerging organic materials. We then systematically discuss the strategies employed to enhance the electrochemical performance (output voltage, capacity, cycling stability, and rate performance) of organic electrode materials in various metal-ion batteries (LIBs, SIBs, KIBs, MIBs, ZIBs, AIBs, and CIBs). Finally, the key challenges and future perspectives of organic electrode materials for metal-ion batteries are also discussed.

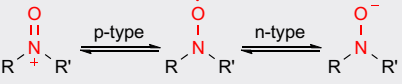
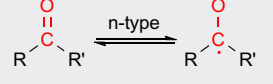
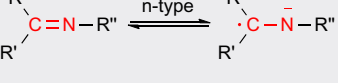
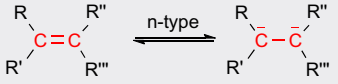
OVERVIEW OF ORGANIC ELECTRODE MATERIALS

The reported organic electrode materials mainly include conductive polymers, organosulfur compounds, organic radicals, carbonyl compounds, and other molecules based on C=N, C≡N, N=N, and multiple carbon bonds (C=C and C≡C). Their redox mechanisms, and related advantages and disadvantages are summarized in Table 1. Generally, the redox reactions of organic electrode materials are based on the charge-state change of the electroactive groups. According to the charge-state change of active sites, organic electrode materials are often classified into three different types: n-type, p-type, and bipolar type.⁷ N-type organic molecules (e.g., quinones) will be reduced to yield anions and then combine with metal ions such as Li⁺ and Na⁺ ions during the discharge process. Different from n-type organic molecules, p-type organic materials (e.g., thioethers) can be oxidized and then interact with anions such as PF₆⁻ and ClO₄⁻. Additionally, organic molecules belonging to bipolar type (e.g., organic radicals) can be reduced or oxidized, which depends on the applied voltage. To understand the fundamental properties of various organic electrode materials clearly, we compare them in the form of radar plots (Figure 1), where their capacity, solubility, preparation complexity, thermal stability, kinetics, voltage, conductivity, and self-discharge are considered. In the following sections, we succinctly discuss these types of organic electrode materials.

¹State Key Laboratory of Elemento-Organic Chemistry and Key Laboratory of Advanced Energy Materials Chemistry (Ministry of Education), College of Chemistry, Nankai University, Tianjin 300071, China

*Correspondence: chenabc@nankai.edu.cn
<https://doi.org/10.1016/j.chempr.2018.09.005>

Table 1. Summary of Redox Mechanisms and Characteristics of Different Types of Organic Electrode Materials

Type	Materials	Redox Mechanism	Advantages	Disadvantages
Conductive polymers	polyacetylene, polyaniline, polypyrrole, polythiophene	$\left(-R \right)_n^{x+} \xrightleftharpoons{p\text{-type}} \left(-R \right)_n \xrightleftharpoons{n\text{-type}} \left(-R \right)_n^{y-}$	high conductivity	low capacity, sloping plateau
Organosulfur compounds	disulfides, polysulfides	$R-S-S-R' \xrightleftharpoons{n\text{-type}} R-S^- + S^{\cdot}-R'$	high capacity	high solubility, ^a low kinetics, low conductivity
	thioethers	$R-S-R' \xrightleftharpoons{p\text{-type}} R-\overset{\cdot}{S}-R'$		
Organic radicals	TEMPO derived, PROXYL derived, nitronyl nitroxide		fast kinetics, flat plateau	low capacity, low conductivity, high self-discharge, high solubility ^a
	phenoxy, galvinoxyl	$Ar-O^{\cdot} \xrightleftharpoons{n\text{-type}} Ar-O^-$		
Carbonyl compounds	quinones, carboxylates, anhydrides, imides, ketones		high capacity, fast kinetics	high solubility, ^a low conductivity
Others	Schiff bases, pteridine derived, phenazine derived		high capacity, fast kinetics	high solubility, ^a low conductivity
	cyano derived	$R-C\equiv N \xrightleftharpoons{n\text{-type}} R-\overset{\cdot}{C}\equiv N$		
	azo compounds	$R-N=N-R' \xrightleftharpoons{n\text{-type}} R-\overset{\cdot}{N}-\overset{\cdot}{N}-R'$		
	multiple carbon bonds			

TEMPO, 2,2,6,6-tetramethylpiperidinyl-N-oxyl; PROXYL, 2,2,5,5-tetramethylpyrrolidin-N-oxyl.

^aThe dissolution behavior in aprotic electrolyte. Carboxylates and carbonyl-based polymers often show low solubility in aprotic electrolyte.

Conductive Polymers

Conductive polymers can store charge through delocalization along their backbone. Most reported conductive polymers that serve as the electrodes are polyacetylene, polyaniline (PAn), PPy, polythiophene, and polyparaphenylenes (PPP).^{4,7} For instance, PPP shows two pairs of well-defined redox peaks in the voltage range of 0.02–1.5 V and 3.9–4.5 V (versus Li⁺/Li), corresponding to the Li⁺ doping (n-type) and PF₆⁻ doping (p-type) reactions, respectively.¹⁶ Although conductive polymers show high electronic conductivity, they still suffer from two main issues. The first problem is that their charge-discharge curves are very sloping because their charged centers are not separated electronically. Another problem is their low available doping levels (at most 0.3 to 0.5), leading to limited capacity (generally less than 100 mAh g⁻¹) in metal-ion batteries such as ZIBs and AlBs.^{7,17,18} Although their capacity could be enhanced by the optimization of morphology, copolymerization, and doping with anions,^{13,19} the energy density of conductive polymers is still relatively low. Thus, more strategies can be developed to further improve their practical capacity in the future.

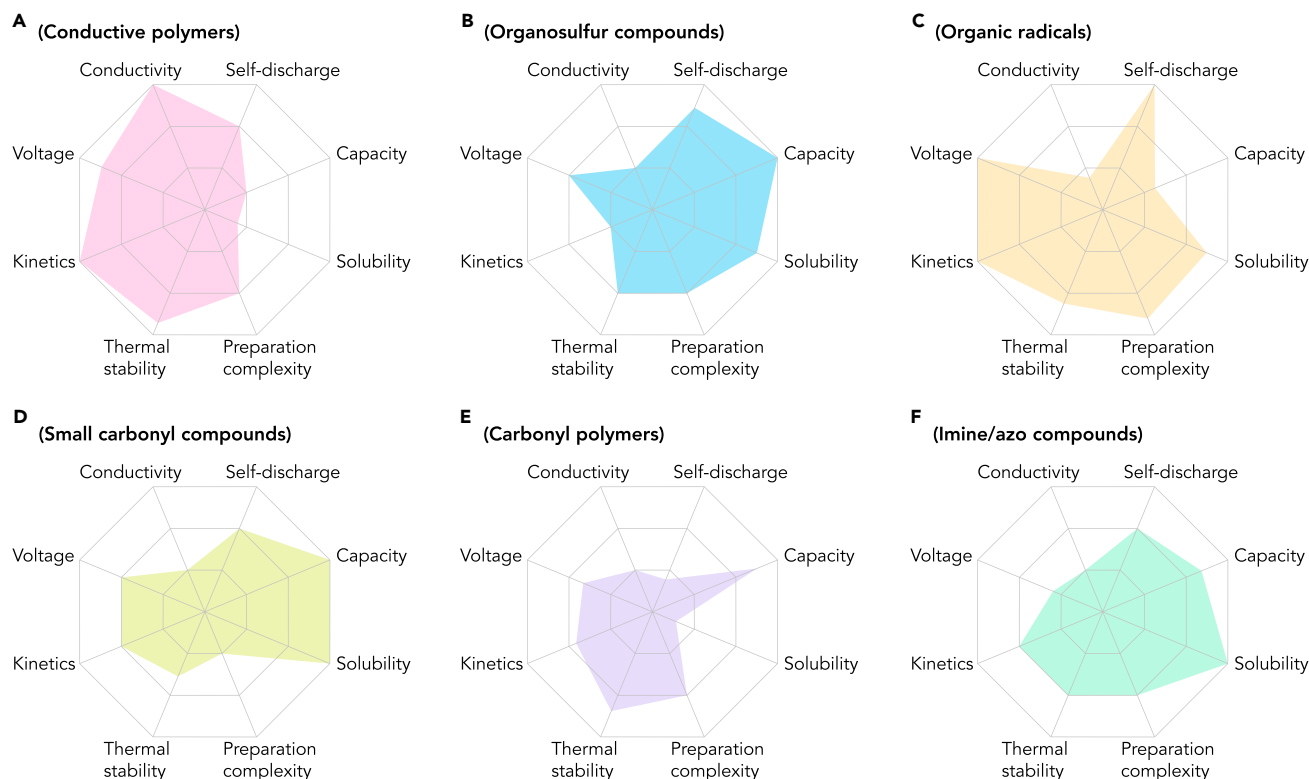


Figure 1. Overview of Fundamental Properties of Different Types of Organic Electrode Materials

The solubility refers to the dissolution behavior of organic materials in aprotic electrolyte. Organic salts with high polarity generally exhibit low solubility.
(A) Conductive polymers; the voltage is based on p-doping reaction.

(B) Organosulfur compounds.

(C) Organic radicals; the voltage is based on p-type reaction.

(D) Small carbonyl compounds; carboxylates often show low working voltage.

(E) Carbonyl polymers.

(F) Imine and azo compounds, including redox centers based on C=N and N=N bonds.

Organosulfur Compounds

Compared with conductive polymers, organosulfur compounds generally show higher capacity. The reported organosulfur compounds mainly cover disulfides, polysulfides, and thioethers. The redox mechanism of disulfides and polysulfides is the reversible breakage and formation of S-S bonds, delivering relatively high theoretical capacity (mostly more than 200 mAh g⁻¹).²⁰ However, because of the poor rebonding efficiency during charge processes, their reaction rate is slow and the electrochemical polarization is large in metal-ion batteries such as MIBs.²¹ In addition, they are plagued by serious dissolution in aprotic electrolyte, leading to fast capacity decay. Unlike disulfides and polysulfides, the redox processes of thioethers (p-type) are not accompanied by the breakage of bonds. The first reported thioethers are poly(2-phenyl-1,3-dithiolane) and poly[1,4-di(1,3-dithiolan-2-yl)benzene] (PDDTB), both of which exhibit an average discharge voltage of 2.2 V (versus Li⁺/Li).²² The PDDTB could deliver a capacity of 378 mAh g⁻¹ at the third cycle and be maintained at 300 mAh g⁻¹ over 20 cycles. Their cycling stability still needs to be further enhanced.

Organic Radicals

Similar to thioethers, the redox process of organic radicals is accompanied by small structure change and electron rearrangement.¹⁰ Therefore, organic radicals

generally exhibit fast kinetics and low voltage polarization. For example, aqueous Zn-radical batteries could operate at a high rate of 60 C with low overpotential (<0.1 V).²³ Moreover, they also show relatively flat charge-discharge plateaus. Since Nakahara et al. first reported the application of poly(2,2,6,6-tetramethylpiperidinyloxy methacrylate) (PTMA) as the cathode for LIBs,¹⁰ organic radicals have attracted extensive attention in recent years. The active redox center of PTMA is 2,2,6,6-tetramethylpiperidinyl-N-oxyl (TEMPO). TEMPO exhibits bipolar properties, which can be either reduced to aminoxy anions or oxidized to oxoammonium cations through a one-electron reaction at low (about 2 V versus Li⁺/Li) or high (above 3 V versus Li⁺/Li) voltage range, respectively.^{7,10} Like PTMA, most reported organic radicals are based on the nitroxyl groups, including TEMPO, 2,2,5,5-tetramethylpyrrolidin-N-oxyl, and nitronyl nitroxide units.^{7,24} Although the discharge voltage of p-type organic radicals is high, their practical discharge capacities are only about 100 mAh g⁻¹ or even lower because of the limited electron transfer number per weight. N-type galvinoxyl and phenoxy radicals were usually applied as the anode materials for aqueous/non-aqueous batteries.^{25,26} Their capacities are lower than those of nitroxyl radicals because of the larger molecular weight of their units. Moreover, they suffer from low intrinsic conductivity and a self-discharge problem, which are the common challenges for organic radicals.

Carbonyl Compounds

Among all reported organic electrode materials, carbonyl compounds (quinones, carboxylates, anhydrides, imides, and ketones) are the most widely studied because of their high capacity and fast kinetics.¹³ In general, they can store charges (n-type) at moderate voltage range (below 3 V versus Li⁺/Li) with high capacity. The simplest quinone (1,4-benzoquinone, BQ) can exhibit average discharge voltage at about 2.7 V (versus Li⁺/Li) and theoretical capacity of 496 mAh g⁻¹, which is more superior than the conventional LiCoO₂ cathode (3.9 V × 155 mAh g⁻¹).²⁷ However, small carbonyl compounds generally suffer from severe dissolution in aprotic electrolyte. Moreover, although they show low solubility in aqueous electrolyte, their discharge products can dissolve in H₂O easily. As a result, their capacity often seriously degrades in aqueous and non-aqueous metal-ion batteries (e.g., MIBs and CIBs) during cycles.²⁸ Moreover, their electronic conductivity is intrinsically inferior, which would restrict the rate performance. If their cycling stability and rate performance could be enhanced effectively, carbonyl compounds would be promising candidates for metal-ion batteries because of their high capacity.

Other Compounds

In addition to the conventional organic electrode materials mentioned above, some organic compounds based on C=N, C≡N, N=N, and multiple carbon bonds (C=C, C≡C) that are usually n-type have been proved to be feasible for metal-ion batteries.¹³ The reported organic electrode materials based on C=N mainly include Schiff bases, pteridine derivatives, and phenazine derivatives.^{29–31} For example, Schiff bases with common repeated Hückel units (–N=CH–R–HC=N–, R is aromatic group) generally show low discharge voltage (<1 V versus Na⁺/Na), indicating that they would be the candidate of anode materials,²⁹ while pteridine derivatives such as alloxazine could be applied as the cathode materials for LIBs thanks to their relatively high discharge voltage (>2 V versus Li⁺/Li).³⁰ Similar to organic materials with C=N groups, n-type compounds based on C≡N (e.g., 9,10-dicyanoanthracene) and N=N (e.g., azobenzene-4,4'-dicarboxylic acid lithium salt [ADALS]) have been reported for metal-ion batteries.^{32–34} It is noteworthy that if multiple carbon bonds (such as C=C and C≡C) of compounds can store Li⁺ ions at low voltage range (mostly <1 V versus Li⁺/Li, superlithiation), their reversible capacity will be very

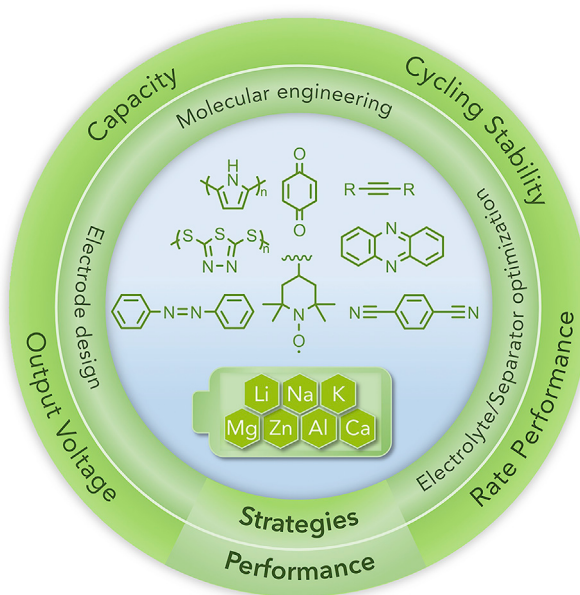


Figure 2. Evaluation Parameters of Various Organic Electrode Materials and Design Strategies in Metal-Ion Batteries

high.^{35,36} Whether the superlithiation of C=C and C≡C could occur depends on the molecular structure and the test conditions. Like simple quinones, the dissolution issue and electronic conductivity should be considered when applying these emerging organic materials for metal-ion batteries.

DESIGN STRATEGIES IN ORGANIC BATTERIES

Battery systems are usually evaluated by three main parameters: energy density, power density, and cycling life. The energy density of batteries depends on their output voltage and capacity. The output voltage and rate capability determine their power density. Thus, it is important to enhance these parameters (output voltage, capacity, cycling stability, and rate performance) of organic electrode materials through molecular engineering, electrode design, and electrolyte and separator optimization (Figure 2). In this section, we mainly focus on the design strategies employed to enhance the electrochemical performance of organic electrode materials in various metal-ion batteries.

Output Voltage

The relationship between the output voltage and energy density of batteries can be described as³⁷

$$E_d = E \times Q \quad (\text{Equation 1})$$

$$E = E_+ - E_-, \quad (\text{Equation 2})$$

where E_d is the energy density, E is the output voltage, Q is the specific capacity, and E_+ and E_- are the operating potentials of the cathode and anode, respectively. According to Equation 1, enhancing output voltage will be helpful in achieving high energy density. For the realization of high output voltage, cathode materials with high operating potential and anode materials with low operating potential are

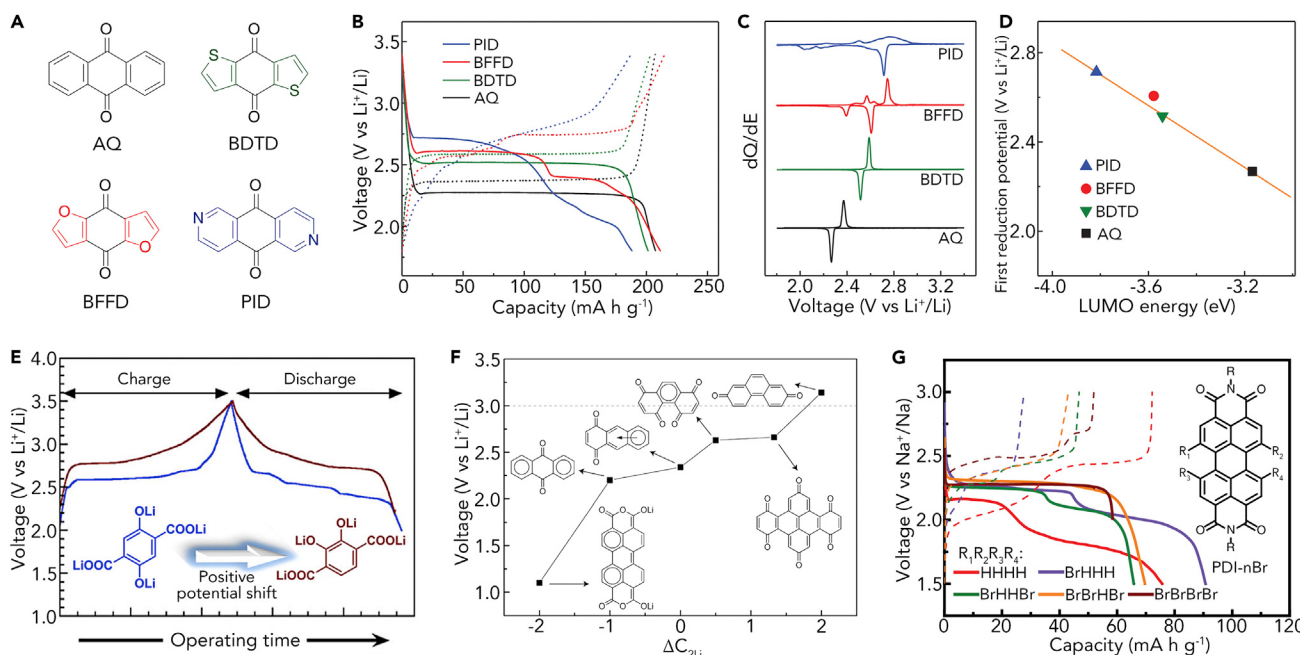


Figure 3. Different Methods of Adjusting the Output Voltage

(A–D) Structural formulas (A), charge-discharge curves (B), differential capacity profiles (C), and relationship between the first discharge potentials and the calculated LUMO energies (D) of AQ, BDTD, BFFD, and PID. Reprinted with permission from Liang et al.³⁸ Copyright 2013 Wiley-VCH Verlag GmbH & Co. KGaA.

(E) Charge-discharge curves of the dihydroxyterephthaloyl derivatives with two -OLi in para and ortho positions. Reprinted with permission from Gottis et al.⁴⁶ Copyright 2014 American Chemical Society.

(F) Correlation between discharge voltage and $\Delta C_{2\text{Li}}$ of some representative carbonyl compounds. Reprinted with permission from Wu et al.⁴⁸ Copyright 2015 Royal Society of Chemistry.

(G) Charge-discharge curves of PDI and its derivatives with different number (1–4) of Br substitutions. Reprinted with permission from Banda et al.⁴⁹ Copyright 2017 Wiley-VCH Verlag GmbH & Co. KGaA.

desired, as suggested by [Equation 2](#). P-type organic materials such as organic radicals and thioethers often exhibit high working potentials. As a result, they are usually used as the cathodes of metal-ion batteries (e.g., aqueous ZIBs).^{19,23} In contrast, n-type organic materials such as carbonyl compounds generally show lower operating potentials (<3 V versus Li⁺/Li). They can serve not only as the cathode but also as the anode, depending on their practical working potentials. Working potentials of organic electrode materials are directly related to their molecular structure. There are many molecular engineering approaches to tune their working potentials.

The introduction of electron-withdrawing groups (e.g., -CF₃, -CN, -F, -Cl, -Br, and -SO₃Na) and electron-donating groups (e.g., -NH₂, -CH₃, -OCH₃, -OLi, and -ONa) is the common way to tune the working potentials of organic materials, since these groups can adjust the energy level of lowest unoccupied molecular orbital (LUMO).³⁸ Low LUMO energy level means high electron affinity, resulting in high working potential. For instance, by introducing electron-withdrawing atoms (S, O, and N) to 9,10-anthraquinone (AQ), our group designed three organic molecules, benzo[1,2-b:4,5-b']dithiophene-4,8-dione (BDTD), benzofuro[5,6-b]furan-4,8-dione (BFFD), and pyrido[3,4-g]isoquinoline-5,10-dione (PID; [Figure 3A](#)).³⁸ As shown in [Figures 3B](#) and [3C](#), the first reduction potentials of BDTD (2.52 V), BFFD (2.61 V), and PID (2.71 V) are higher than that of AQ (2.27 V). The results are well consistent with theoretical calculations ([Figure 3D](#)), where the first reduction potentials exhibit

a linear correlation with the corresponding calculated LUMO energies. In contrast, carboxylates with electron-donating groups (such as $-OLi$) generally exhibit low discharge potentials and can be used as anode materials.³⁹ To understand clearly how functional groups affect the working potential, we summarize the potential change of BQ or naphthoquinone (NQ) after introducing the common groups (Table 2).^{40–45} In addition to the intrinsic properties of substituent groups, their number can also affect the working potentials.⁴¹ Moreover, the working potentials of organic materials can be tuned by the relative position of active groups.^{46,47} For instance, in the dihydroxyterephthaloyl systems, the discharge potential exhibits a positive shift of about 300 mV from the *para* to *ortho* position of active groups because of the favorable Coulombic interaction (Figure 3E).⁴⁶

In addition, theoretical analysis indicates that it is feasible to tune working potential of organic molecules by designing a different conjugated structure. For example, Wu et al. studied the relationship between the electron delocalization (aromaticity) and the discharge potential of carbonyl containing polycyclic aromatic hydrocarbons.⁴⁸ The results reveal that high discharge potential would be achieved if the aromaticity increases after lithiation. The aromaticity change after lithiation can be expressed by an index (ΔC_{2Li}), which obeys the equation⁴⁸

$$\Delta C_{2Li} = \frac{\Delta C}{0.5 \times \Delta Li}, \quad (\text{Equation 3})$$

where ΔC_{2Li} is the average change of Clar sextet numbers after two Li atoms are absorbed, ΔC is the change of Clar sextet numbers during lithiation, and ΔLi is the number of adsorbed Li atoms. According to Equation 3, the ΔC_{2Li} of some representative organic molecules can be obtained (Figure 3F). In particular, the theoretical discharge voltage of phenanthrene-2,7-dione (Figure 3F) could exceed 3 V (versus Li^+/Li) because of the large positive value of ΔC_{2Li} .

In general, the flat discharge plateau is beneficial for achieving stable voltage output. Therefore, it is meaningful to tune the shape of the discharge curve through molecular engineering. Banda et al. designed five perylene diimides (PDI, PDI-1Br, PDI-2Br, PDI-3Br, and PDI-4Br) with different dihedral angles by adjusting the number of Br (Figure 3G).⁴⁹ The dihedral angles exhibit a gradual increase from PDI to PDI-4Br according to their optimized structures. As shown in Figure 3G, PDI, PDI-1Br, and PDI-2Br show two discharge plateaus, whereas both PDI-3Br and PDI-4Br exhibit one stable discharge platform, implying that the angles between two planes in organic molecules can affect the shape of their discharge curves.

Capacity

High specific capacity is helpful in achieving high energy density (Equation 1). The theoretical capacity of electrode materials can be calculated as³⁷

$$Q = \frac{nF}{3.6M_w}, \quad (\text{Equation 4})$$

where Q is the specific capacity (mAh g^{-1}), n is the number of transferred electrons of one molecule, F is the Faraday constant (C mol^{-1}), and M_w is the molecular weight (g mol^{-1}). Take AQ as an example (Figure 4A): AQ with a molecular weight of 208.2 g mol^{-1} can undergo a two-electron reaction, resulting in a theoretical capacity of 257 mAh g^{-1} . In this section, we discuss how to design organic molecules with high theoretical capacity and then achieve the theoretical values in detail.

Table 2. Summary of the Working Voltage Change (ΔE) after Introduction of the Representative Electron-Withdrawing and -Donating Groups (Marked in Red)

Electron-Withdrawing Groups	$-\text{CF}_3$	$-\text{CN}$	$-\text{F}$	$-\text{Cl}$	$-\text{Br}$	$-\text{SO}_3\text{Na}$
Examples						
ΔE^{a} (V)	+0.3 ⁴⁰	+0.6 ⁴⁰	+0.5 ⁴¹	+0.3 ⁴¹	+(0–0.3) ⁴¹	+0.2 ⁴²
Electron-Donating Groups	$-\text{CH}_3$	$-\text{OCH}_3$	$-\text{NH}_2$	$-\text{Ph}$	$-\text{OLi}$	$-\text{ONa}$
Examples						
ΔE^{a} (V)	-0.1 ⁴⁰	-0.1 ⁴⁰	-0.2 ⁴³	-0.3 ⁴²	-0.9 ⁴⁴	-1.2 ⁴⁵

^a ΔE values are based on the average discharge voltage of each molecule and the corresponding unsubstituted molecule (BQ or NQ).

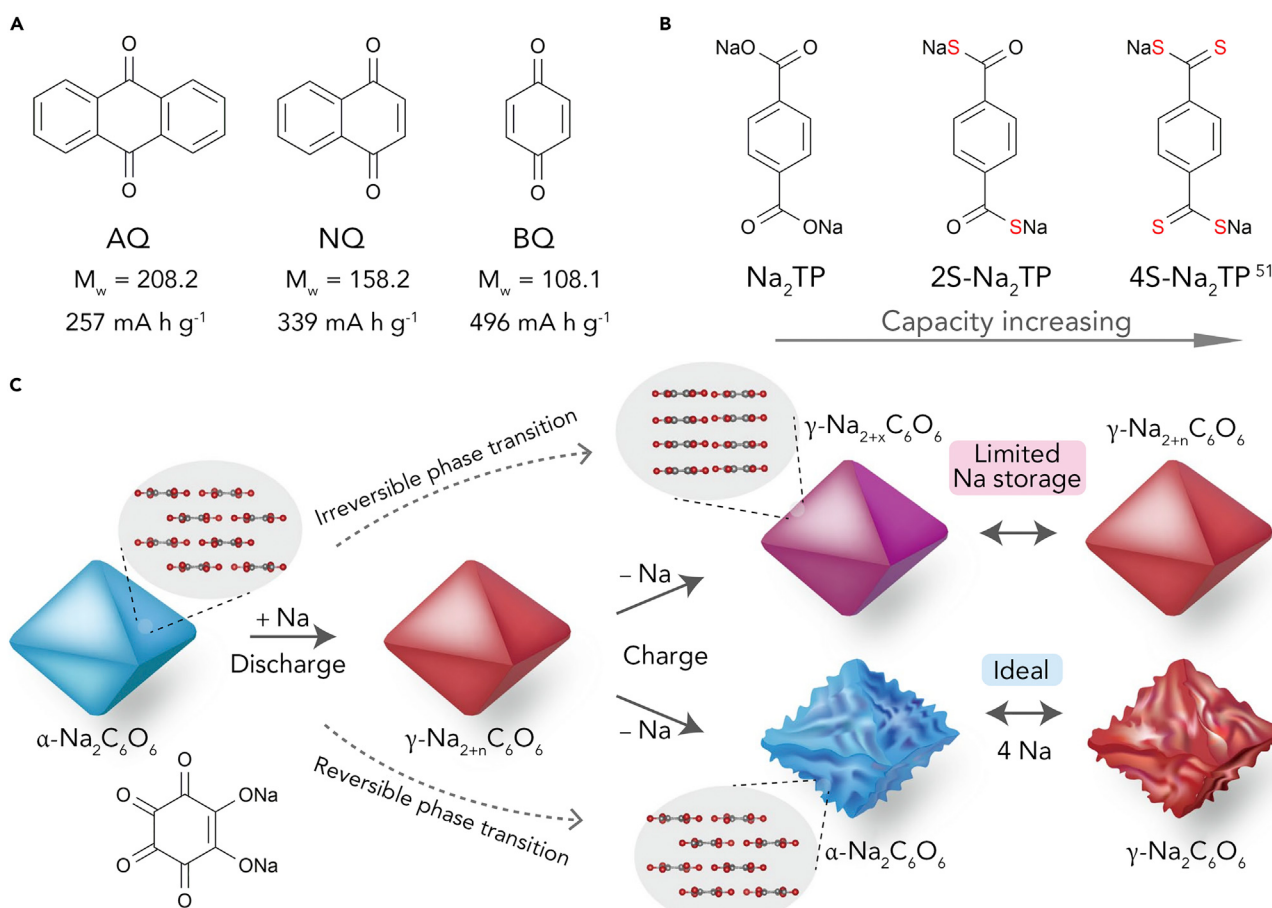


Figure 4. Different Approaches to Increasing the Capacity

(A) Structural formula, molecular weight, and theoretical capacity of AQ, NQ, and BQ.

(B) Structural formulas of Na_2TP , $2\text{S-Na}_2\text{TP}$, and $4\text{S-Na}_2\text{TP}$.

(C) Schematic diagram of the proposed sodiation and desodiation mechanism of $\text{Na}_2\text{C}_6\text{O}_6$ with irreversible or reversible phase transformation. Reprinted with permission from Lee et al.⁵⁰ Copyright 2017 Springer Nature.

According to Equation 4, higher theoretical capacity can be achieved by designing organic materials with more redox-active sites and lower molecular weight. As shown in Figure 4A, the molecular weight gradually increases from BQ to NQ to AQ, and they all undergo two-electron reactions. Thus, their theoretical capacity follows the order BQ > NQ > AQ. The theoretical number of electrons transferred depends on the structure of organic molecules. For example, the disodium salt of terephthalate (Na_2TP) can undergo two-electron transfer, corresponding to a theoretical capacity of 255 mAh g^{-1} . When the O atoms are replaced by S atoms, the capacity will increase dramatically because of the enhanced electron delocalization and conductivity. In particular, the full S-substituted compound (sodium tetrathioterephthalate, $4\text{S-Na}_2\text{TP}$; Figure 4B) can store six electrons per molecule, corresponding to a high theoretical capacity of 586 mAh g^{-1} .⁵¹ The high capacity is derived from the extra Na^+ -ion uptake by the aromatic rings, whose electron density improves after S substitution. This work reveals that the number of electrons accepted by organic compounds (such as the superlithiation of C=C) can be adjusted via proper molecular design.

After optimizing theoretical capacity, the following issue is how to achieve practical capacity as close as possible to the theoretical value. The practical capacity of

organic materials can be influenced by many factors such as crystallinity, particle size, conductive additives (e.g., their ratio and electronic conductivity), electrolyte, and measurement conditions (e.g., current density and voltage range).^{12,52} For example, the initial discharge capacity of amorphous polypyrene is much higher than that of crystalline pyrene (92 versus 20 mAh g⁻¹) in AlBs because the effective insertion of AlCl₄⁻ needs a large intermolecular distance.⁵² Generally, the small particle size of organic materials is helpful in improving their practical capacity. However, the dissolution problem may become more serious with the decreased size of active materials. Additionally, more carbon additives with superior conductivity will contribute to realizing higher practical capacity because of the inferior electronic conductivity of most organic materials. Nevertheless, too many carbon additives would inevitably lead to decreased energy density of the whole batteries.

The practical capacity of organic materials can also be affected by their phase transformation during the charge-discharge process. For instance, Bao and coworkers studied the phase transformation of disodium rhodizonate (Na₂C₆O₆) during charge-discharge processes.⁵⁰ As shown in Figure 4C, the initial α phase of Na₂C₆O₆ can transform into the γ phase easily during the sodiation process, whereas the transformation from the γ phase to the α phase is kinetically suppressed in the following desodiation process. The irreversible phase transformation leads to low practical capacity. By reducing the particle size, optimizing electrolyte (diethylene glycol dimethyl ether), and controlling charge voltage to realize reversible phase transformation between the α and γ phases (Figure 4C), Na₂C₆O₆ could deliver a reversible capacity of 484 mAh g⁻¹, which is very close to the theoretical value (501 mAh g⁻¹, 4Na). This work provides a valuable strategy to reach the theoretical capacity of organic materials.

Cycling Stability

Cycling stability is also an important aspect for the application of organic electrode materials in metal-ion batteries. Organic materials, especially small organic molecules, often show poor cycling stability because of their high solubility, their discharge products, or both in electrolyte. Moreover, the dissolution problem will lead to side reactions, self-discharge problems, and low Coulombic efficiency. In addition to the dissolution issue, other factors such as volume change, pulverization of active materials, phase transformation, and the instability of intermediates would also bring about poor cycling stability. Many strategies have been reported to enhance the cycling stability, including polymerization, salification, hybridization with insoluble materials, optimization of electrolyte, and other methods such as separator modification.

Polymerization

Combining small molecules to form polymers is an effective way to enhance the cycling stability because of the limited solubility of polymers in aqueous and non-aqueous electrolyte.^{4,7,19} For instance, the capacity of small molecule (3,4,9,10-perylenetetracarboxylic dianhydride) fades rapidly in aqueous MIBs and CIBs.²⁸ In contrast, the anhydride-derived polyimide exhibits high capacity retention of 88% after 1,000 cycles in aqueous CIBs.⁵³ Similar results can also be found in aqueous AlBs and MIBs.^{52,54} It is noteworthy that the solubility of polymers in electrolyte is closely related to their practical molecular weights and the property of electrolyte.^{55–58} For example, Zhang et al. synthesized organic radical poly(TEMPO methacrylate) (PTOMA) with different degrees of polymerization from 66 to 703 (Figure 5A).⁵⁵ As shown in Figure 5B, the cycling stability of PTOMA

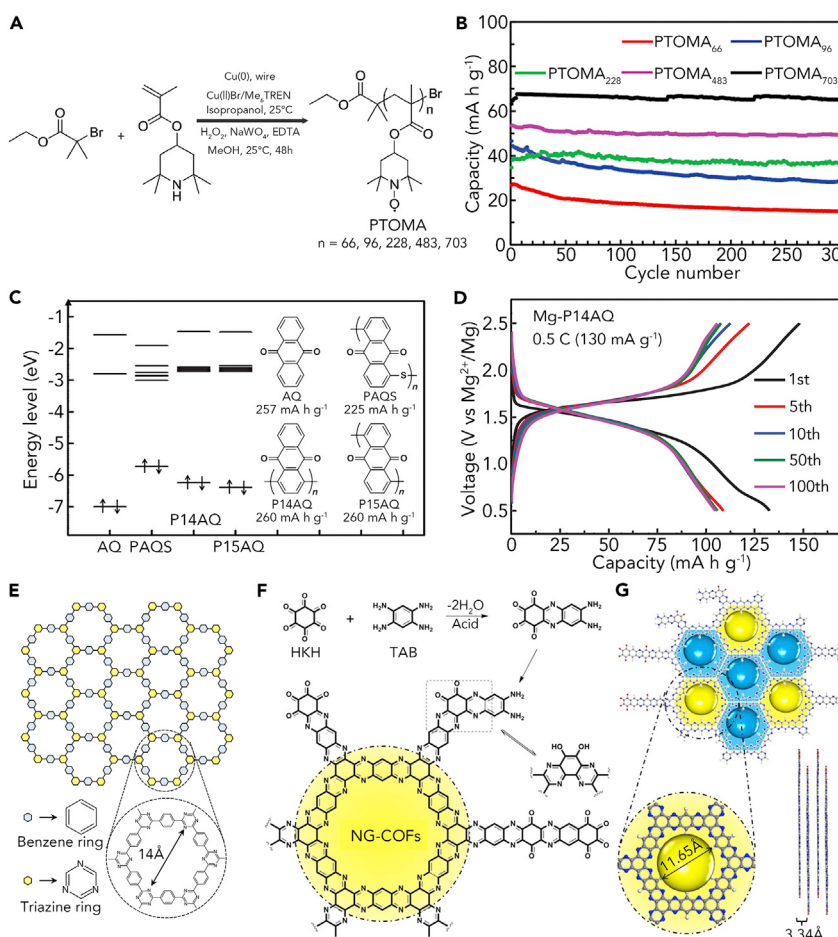


Figure 5. Improvement of Cycling Stability by Polymerization

(A and B) Synthetic route (A) and cycling performance (B) of PTOMA with different molecular weights. Reprinted with permission from Zhang et al.⁵⁵ Copyright 2017 Royal Society of Chemistry. (C) Electron configuration, structural formula, and theoretical capacity of AQ, PAQS, P14AQ, and P15AQ. Reprinted with permission from Song et al.⁵⁶ Copyright 2015 Wiley-VCH Verlag GmbH & Co. KGaA.

(D) Charge-discharge curves of P14AQ at 0.5 C (130 mA g⁻¹). Reprinted with permission from Pan et al.⁵⁸ Copyright 2016 Wiley-VCH Verlag GmbH & Co. KGaA.

(E) Structural illustration of the COFs consisting of benzene and triazine rings with a pore diameter of 14 Å. Reprinted with permission from Sakaushi et al.⁵⁹ Copyright 2013 Springer Nature.

(F and G) Schematic representation of the NG-COFs (F) and a single layer with pore size of 11.65 Å and packing distance of 3.34 Å (G). Reprinted from Lin et al.⁶⁰

in LIBs is enhanced with the increase of polymerization degrees, implying that larger molecular weight of polymer results in lower solubility in electrolyte. Analogously, compared with poly(1,4-anthraquinone) (P14AQ; Figure 5C), the cycling performance of poly(1,5-anthraquinone) (P15AQ) in LIBs is unsatisfactory because of its low molecular weight (about 2,300).⁵⁶ In addition to the pristine polymers, the dissolution issue of the intermediates during the charge-discharge process could also affect the cycling stability. For instance, the dissolution of discharged poly(anthraquinonyl sulfide) (PAQS) is serious in dimethylformamide-based Mg electrolyte, leading to fast capacity decay.^{57,58} In contrast, P14AQ shows good cycling performance in MIBs (Figure 5D) attributable to the limited solubility of the intermediates.⁵⁸ Although the cycling stability of small carbonyl compounds could be enhanced by polymerization, the obtained polymers generally exhibit lower

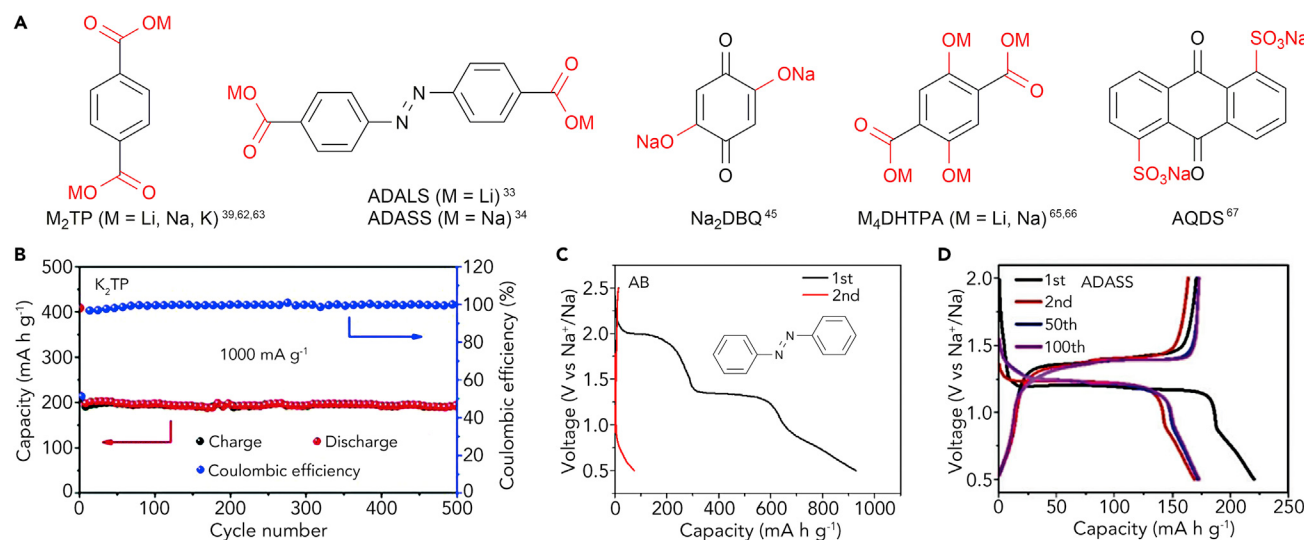


Figure 6. Improvement of Cycling Stability by Salification

(A) Structural formula of M₂TP (M = Li, Na, K), ADALS, ADASS, Na₂DBQ, M₄DHTPA (M = Li, Na), and AQDS.

(B) Cycling performance of K₂TP at 1 A g⁻¹. Reprinted with permission from Lei et al.⁶² Copyright 2017 Royal Society of Chemistry.

(C and D) Charge-discharge curves of AB (C) and ADASS (D) at 0.2 C. Reprinted with permission from Luo et al.³⁴ Copyright 2018 Wiley-VCH Verlag GmbH & Co. KGaA.

discharge voltage than corresponding monomers, and their charge-discharge curves become sloping.^{56,58} Moreover, the practical capacity of polymers is usually lower than the theoretical value because of the limited utilization of active sites.⁷

Compared with conventional polymers, two-dimensional (2D) conjugated polymers such as covalent organic frameworks (COFs) generally possess high specific area and porous structure. As a result, they often exhibit high activity in metal-ion batteries. For example, COFs (Figure 5E), which consist of benzene and triazine rings, can serve as the electrode of SIBs and display high capacity retention of 80% over 7,000 cycles.⁵⁹ In addition, Zhang's group prepared well-defined single-layer 2D nitrogen-rich graphene-like COFs (NG-COFs; Figure 5F).⁶⁰ The single-layer NG-COFs with 11.65 Å in micropores and a packing distance of 3.34 Å are shown in Figure 5G. As anode materials for LIBs, the NG-COFs exhibit high reversible capacity of 1,320 mAh g⁻¹ at 20 mA g⁻¹ and long cycling life of 600 cycles. However, the redox mechanism during the charge-discharge processes needs to be investigated. Additionally, the electrochemical performance of COFs in different metal-ion batteries such as LIBs, KIBs, and MIBs require further study.⁶¹

Salification

Introducing high-polarity groups into organic materials to form organic salts can also enhance their cycling stability because of the limited dissolution in aprotic electrolyte. The groups with high polarity mainly include -COOM (M represents metals such as Li, Na, and K), -OM, and -SO₃Na. Some typical organic molecules with these functional groups have been used in metal-ion batteries, as listed in Figure 6A. However, since they tend to dissolve in aqueous electrolyte, they would be not suitable for application in aqueous metal-ion batteries.

Tarascon's group first reported the conjugated Li₂TP as anode materials for LIBs in 2009.³⁹ Subsequently, Na₂TP and K₂TP were applied in SIBs and KIBs, respectively.^{62,63} Thanks to the high polarity of -COOK, K₂TP could exhibit a high capacity

retention of 94.6% over 500 cycles at 1 A g^{-1} with a Coulombic efficiency of 100% (*Figure 6B*).⁶² Analogously, to inhibit the dissolution of azobenzene (AB) in electrolyte, Luo et al. introduced two $-\text{COOM}$ ($\text{M} = \text{Li}, \text{Na}$) groups to the structure of AB, forming ADALS or azobenzene-4,4'-dicarboxylic acid sodium salt (ADASS).^{33,34} As shown in *Figures 6C* and *6D*, the cycling stability of ADASS is much better than that of AB, demonstrating the effective function of $-\text{COONa}$ toward mitigating dissolution. A similar result can be obtained by introducing $-\text{COOLi}$ to AB for application in LIBs.³³

Organic materials with $-\text{OM}$ groups also show limited dissolution in aprotic electrolyte. For instance, disodiated 2,5-dihydroxy-1,4-benzoquinone (Na_2DBQ ; *Figure 6A*) without extra modification could exhibit long cycle life up to 300 cycles.⁴⁵ A similar result can be obtained in Mg-Li dual-ion batteries with $\text{Na}_2\text{C}_6\text{O}_6$ as the cathode.⁶⁴ By combining $-\text{OM}$ and $-\text{COOM}$ ($\text{M} = \text{Li}, \text{Na}$), both tetrolithium salt of 2,5-dihydroxyterephthalic acid (Li_4DHTPA) and the corresponding tetrasodium salt (Na_4DHTPA) can be used as the cathode and anode materials to construct symmetric batteries.^{65,66} The resultant full SIBs exhibited a capacity retention of 76% after 100 cycles at 0.1 C .⁶⁶ Other groups such as $-\text{SO}_3\text{Na}$ have also been introduced into organic molecules to improve the cycling stability.^{42,67} For example, adding two $-\text{SO}_3\text{Na}$ groups in AQ can form anthraquinone-1,5-disulfonic acid sodium salt (AQDS; *Figure 6A*), which shows better cycling performance than pristine AQ.⁶⁷ However, the introduction of inactive groups with large molecular weight (e.g., $-\text{SO}_3\text{Na}$) will inevitably lead to reduced capacity.

Hybridization with Insoluble Materials

In addition to the aforementioned molecular engineering approaches, combining organic materials with insoluble substrates (e.g., various carbon materials) is also helpful in reducing their dissolution in electrolyte because of the strong interactions between substrates and organic molecules. The interactions include physisorption, chemical bonding, or both. For example, Kang and coworkers combined lumiflavine (LF) with single-walled carbon nanotubes (SWCNTs) through sonication, followed by filtering.⁶⁸ The schematic diagram of π - π interactions between SWCNTs and aromatic structured LF is shown in *Figure 7A*. The physical interactions are confirmed by Raman spectra, where blue shifting occurs in the LF-SWCNTs composites (*Figure 7B*). The composites with 40–50 wt % LF show a high capacity retention of 99.7% after 100 cycles (*Figure 7C*). This method can be extended to other aromatic structured organic molecules such as AQ. However, the cycling performance becomes inferior when the content of LF reaches 60 wt % (*Figure 7C*). In this state, there are some extra LFs that cannot adhere on the surface of SWCNTs to form π - π interactions. Therefore, the shortcoming of this method is the limited mass loading of active materials, which restricts the energy density.^{30,68} This problem can also be found in the composites of graphene and Juglone, where the optimized content of Juglone is only 30.4 wt %.⁶⁹ Encapsulation of organic active materials in CNTs could improve the active mass loading to some extent.⁷⁰ In addition to graphene and CNTs, other insoluble materials such as CMK-3 have also been reported to combine with organic materials to suppress the dissolution issue.⁷¹ Moreover, recent research reveals that the nanoconfinement effect of CMK-3 could alleviate the phase transformation-induced capacity decay of p-chloranil in aqueous ZIBs.⁷²

Compared with physical interactions, covalent grafting of organic molecules on insoluble substrates would be more effective in mitigating the dissolution problem because of the stronger interactions.^{73,74} For instance, Lin et al. fabricated lithium-organic radical batteries by using PTMA-based brush/ SiO_2 composites as cathode,

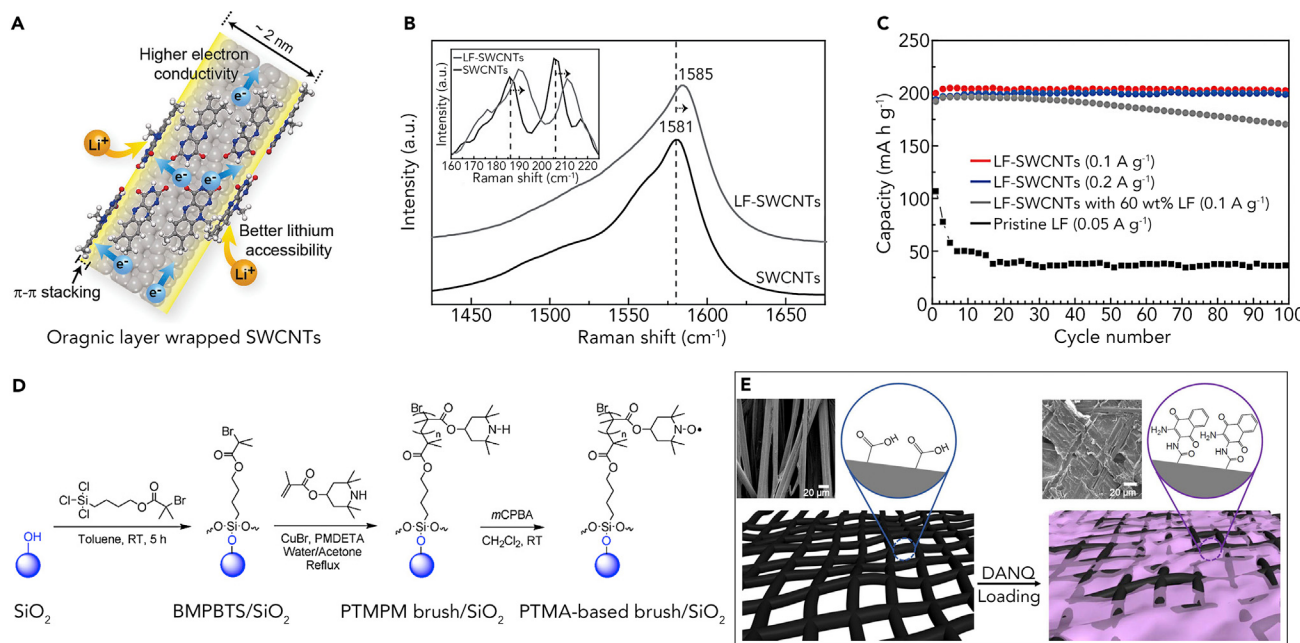


Figure 7. Improvement of Cycling Stability by Hybridization with Insoluble Materials

(A–C) Schematic diagram of π - π stacking between LF and SWCNTs (A), Raman spectra of pristine SWCNTs and LF-SWCNTs composites (B), and cycling performance of pristine LF and LF-SWCNTs composites with different LF contents (C). Reprinted with permission from Lee et al.⁶⁸ Copyright 2014 Wiley-VCH Verlag GmbH & Co. KGaA.

(D) Synthetic route of PTMA-based brush/SiO₂ composites. Reprinted from Lin et al.⁷³

(E) Fabrication process of attaching DANQ on -COOH-based porous current collector; the insets are the corresponding scanning electron microscopy (SEM) images. Reprinted with permission from Lee et al.⁴³ Copyright 2016 American Chemical Society.

whereby the brushes were covalently grafted on SiO₂ nanoparticles (Figure 7D).⁷³

Thanks to the restrained dissolution of active materials, the batteries could exhibit a long cycle life of 300 cycles. However, the insulating SiO₂ may affect the rate performance of batteries. In contrast, using conductive substrates such as carbon black and current collector to fix organic molecules is beneficial in improving the rate capability at the same time. For example, Park's group attached 2,3-diamino-1,4-naphthoquinone (DANQ) on -COOH-based porous current collector through chemical reactions (Figure 7E).⁴³ The composite cathode exhibited long cycling life (500 cycles) and high rate capability of 84 mA h g⁻¹ at 50 C, implying the positive function of covalent grafting between organic molecules and conductive insoluble substrates.

Optimization of Electrolyte

Optimizing the electrolyte is another effective way to enhance the cycling stability of organic electrode materials because the property of electrolyte can directly affect the dissolution behavior. Increasing the concentration of electrolyte and developing quasi- or all-solid-state electrolyte are beneficial in mitigating the dissolution issue. To investigate the effect of electrolyte concentration, our group developed CF₃SO₃Na/triethylene glycol dimethyl ether (TEGDME) with different concentrations of 1, 2, 3, and 4 mol L⁻¹.⁷¹ As shown in Figure 8A, the electrolytes with lower concentration (1–3 mol L⁻¹) turned yellow after 1 day, indicating the dissolution of AQ. In contrast, the color was nearly unchanged even after 10 days in the electrolyte with high salt concentration (4 mol L⁻¹). The batteries with the highest concentration of electrolyte (4 mol L⁻¹) exhibited the best cycling performance (Figure 8B). The

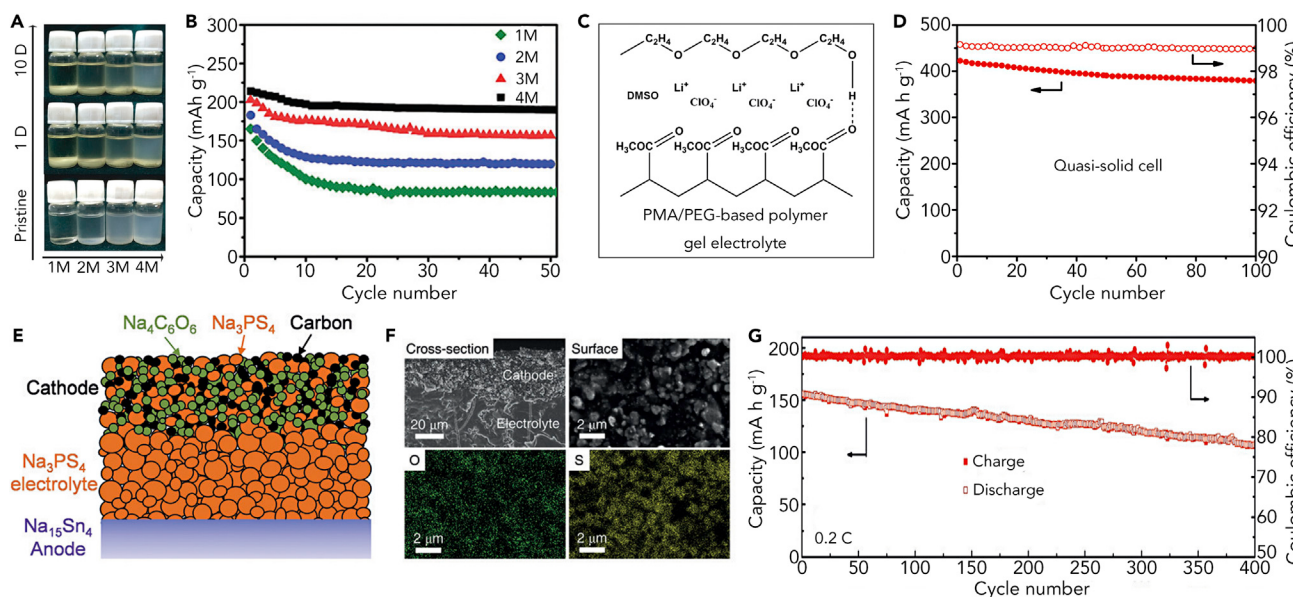


Figure 8. Improvement of Cycling Stability by Optimization of Electrolyte

(A and B) Dissolution behavior (A) and cycling performance (B) of AQ in CF₃SO₃Na/TEGDME electrolyte with different concentrations of 1, 2, 3, and 4 mol L⁻¹. Reprinted with permission from Guo et al.⁷¹ Copyright 2015 Royal Society of Chemistry.

(C and D) Schematic illustration of PMA/PEG-based gel electrolyte (C) and cycling performance of C4Q with the gel electrolyte at 0.2 C (D). Reprinted with permission from Huang et al.⁷⁵ Copyright 2013 Wiley-VCH Verlag GmbH & Co. KGaA.

(E–G) Schematic illustration (E), SEM images and mappings of the cathode and electrolyte (F), and cycling stability of the Na₄C₆O₆|Na₃PS₄|Na₁₅Sn₄ solid-state batteries at 60°C (G). Reprinted with permission from Chi et al.⁷⁶ Copyright 2018 Wiley-VCH Verlag GmbH & Co. KGaA.

design strategy of electrolyte could be extended to enhance the cycling stability of other organic materials.

Similar to electrolyte with high concentration, developing quasi-solid-state electrolyte is also effective in improving the cycling performance of organic materials. For instance, the LIBs with poly(methacrylate) (PMA)/poly(ethylene glycol) (PEG)-based quasi-solid-state electrolyte (Figure 8C) and calix[4]quinone (C4Q) cathode show good capacity retention of 89.8% after 100 cycles (Figure 8D).⁷⁵ However, the PMA/PEG-based electrolyte still contains a liquid component (dimethyl sulfoxide), which might evaporate at high temperature, followed by decreased ionic conductivity of electrolyte. Thus, developing all-solid-state electrolyte for organic batteries is necessary. Recently, Yao's group fabricated all-solid-state SIBs by using Na₃PS₄ as the electrolyte and Na₄C₆O₆ as the cathode (Figure 8E).⁷⁶ Scanning electron microscopy images and corresponding mappings in Figure 8F verify the good contact between organic cathode and electrolyte. The ionic conductivity of Na₃PS₄ electrolyte is 0.39 mS cm⁻¹ at 60°C. The batteries could exhibit a capacity retention of 70% after 400 cycles at 0.2 C (Figure 8G). However, the Na₃PS₄ electrolyte is not suitable for batteries with high-voltage organic cathode materials because its anodic decomposition potential is only 2.7 V (versus Na⁺/Na). Developing all-solid-state electrolyte may be an ultimate way to realize state-of-the-art metal-organic batteries for practical applications if the ionic conductivity, chemical and electrochemical stability, and interface issue of solid-state electrolyte can be addressed properly.

Other Approaches

In addition to the dissolution problem, other issues such as instability of intermediates, volume change, and pulverization could also affect the cycling stability of

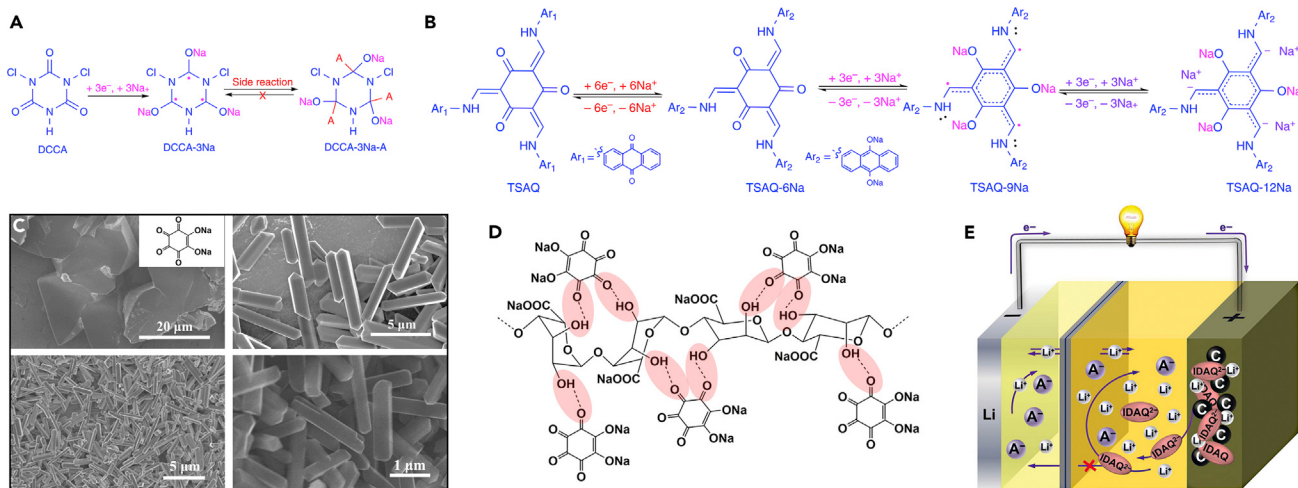


Figure 9. Improvement of Cycling Stability by Other Approaches

(A and B) Sodiation and desodiation mechanisms of DCCA (A) and TSAQ (B). Reprinted from Wu et al.⁷⁷ Licensed under CC BY 4.0.

(C) SEM images of $\text{Na}_2\text{C}_6\text{O}_6$ with different morphologies (microbulk, microrod, and nanorod). Reprinted with permission from Wang et al.⁷⁹ Copyright 2016 American Chemical Society.

(D) Schematic diagram of hydrogen bonds between $\text{Na}_2\text{C}_6\text{O}_6$ and sodium alginate binder. Reprinted from Luo et al.⁸⁰

(E) Schematic illustration of the Li-IDAQ cell configuration with cation-selective sandwich-type separator. Reprinted with permission from Song et al.⁸¹ Copyright 2016 Wiley-VCH Verlag GmbH & Co. KGaA.

organic electrode materials. Many methods have been reported to solve these problems, including designing specific molecular structure, reducing particle size, utilizing multifunctional binders, and modifying separators.

As shown in Figure 9A, DCCA will generate α -C radical intermediate after combining with three Na^+ ions and electrons. Because of the poor stability of the produced radical intermediates, undesired side reactions tend to occur, forming inactive precipitates irreversibly. Thus, the cycling stability of DCCA is rather poor.⁶ To solve this problem, Lu's group utilized resonance and steric effects to design specific organic molecules with stable α -C radical intermediates.⁷⁷ One example is (tris *N*-salicylideneanthraquinoylamine) (TSAQ), which can stabilize the radical intermediates through π - π conjugation, 9- π -electron aromatic Hückel ring, and the steric effect of the rigid geometry (Figure 9B). Therefore, the TSAQ anode could exhibit ultralong cycling life over 2,500 cycles at 1 A g^{-1} . A similar phenomenon can be found in other organic materials. For example, the radical intermediates of poly(3-vinyl-*N*-methylphenothiazine) (PVMPT) are stabilized via π - π interactions, resulting in high capacity retention of 93% after 10,000 cycles at 10 C .⁷⁸ However, the specific capacity of PVMPT is lower than 80 mAh g^{-1} . These works reveal that the stability of intermediates has significant influence on the cycling stability of organic electrode materials.

Although some oxocarbon salts such as rhodizonate salt ($\text{Li}_2\text{C}_6\text{O}_6$, $\text{Na}_2\text{C}_6\text{O}_6$) and croconic acid salt ($\text{Na}_2\text{C}_5\text{O}_5$) are difficult to dissolve in aprotic electrolyte, they still show unsatisfactory cycling performance, which can be ascribed to the large volume change and pulverization of active materials during charge-discharge processes. Among different $\text{Na}_2\text{C}_6\text{O}_6$ samples with microbulk, microrod, and nanorod morphologies (Figure 9C),⁷⁹ the $\text{Na}_2\text{C}_6\text{O}_6$ nanorod shows the best cycling stability because the nanorod structure can mitigate pulverization, improve utilization of active materials, and enhance kinetics. To further enhance the cycling stability of $\text{Na}_2\text{C}_6\text{O}_6$, Wang's group proposed self-healing chemistry between hydroxyl-rich binder (such as sodium alginate) and

oxygen-rich active materials (such as $\text{Na}_2\text{C}_6\text{O}_6$).⁸⁰ The $\text{Na}_2\text{C}_6\text{O}_6$ nanoparticles derived from pulverization during the cycling process can be absorbed by the sodium alginate binder because of the existence of strong hydrogen bonds between them (Figure 9D). Thus, the batteries show long cycling life of 500 cycles with capacity decay of 0.051% per cycle. This work provides an effective way to alleviate the pulverization-induced capacity degradation of oxygen-rich active materials. Additionally, designing specific binders such as conductive poly(3,4-ethylenedioxythiophene):poly(styrenesulfonate) to generate strong interactions with organic active molecules is beneficial in mitigating the dissolution problem.⁸²

In addition to the various molecular engineering and electrode design methods mentioned above, using modified separators has also been proved to be effective in enhancing the cycling stability. For example, Song et al. designed a polypropylene/Nafion/polypropylene sandwich-type separator, which only permits cation migration (Figure 9E).⁸¹ Thus, the shuttle effect induced by the dissolution of organic materials can be eliminated effectively. The LIBs with the modified separator and 1,1'-iminodianthraquinone (IDAQ) cathode exhibit a capacity retention of 76% over 400 cycles and high Coulombic efficiency (>99.6%). Analogously, by means of the cation-selective property of Nafion, our group constructed very stable aqueous Zn-C4Q batteries (up to 1,000 cycles) with Nafion as the separator.⁸³ However, using ion selective separators cannot solve the dissolution issue fundamentally.

Rate Performance

Similar to energy density, power density is also an important parameter in the evaluation of rechargeable batteries, which can be obtained as follows:³⁷

$$P = E \times I, \quad (\text{Equation 5})$$

where P is the power, E is the output voltage, and I is the current. Power density reflects the charge-discharge ability of organic electrode materials at different rates. In the achievement of high power density, the key issue is to enhance rate performance. High rate performance requires fast electron and ion transfer during charge-discharge processes. Clearly, rate performance of organic materials can be affected by many factors, including their intrinsic properties and external conditions (e.g., electrolyte and conductive additives). The favorable intrinsic properties are as follows: fast reaction kinetics of active functional groups, and high conductivity and small particle size of active materials.² In this section, we summarize the approaches used to improve rate performance of organic electrode materials from two aspects, namely molecular engineering and electrode design.

Molecular Engineering

The electron transfer in organic molecules can be enhanced by rational molecular design such as introducing conductive units and extending conjugated structure. For instance, on the basis of the backbone-insulated poly[[N,N' -bis(2-octyldodecyl)-1,4,5,8-naphthalenedicarboximide-2,6-diyl]-*alt*-5,5'-[2,2'-(1,2-ethanediyl)bithiophene]] (P(NDI2OD-TET)), Liang and coworkers designed π -conjugated poly[[N,N' -bis(2-octyldodecyl)-1,4,5,8-naphthalenedicarboximide-2,6-diyl]-*alt*-5,5'-(2,2'-bithiophene)] (P(NDI2OD-T2)) with conductive main chains (Figure 10A).⁸⁴ After more than 20 mol % n-doping, the electronic conductivity of P(NDI2OD-T2) is much higher than that of P(NDI2OD-TET) (10^{-3} versus $10^{-7} \text{ S cm}^{-1}$). Thanks to its highly conductive backbone, P(NDI2OD-T2) could exhibit 95% of its theoretical capacity at an ultrahigh rate of 100 C (72 s per cycle). However, the capacity of P(NDI2OD-T2) is lower than 60 mAh g^{-1} because of

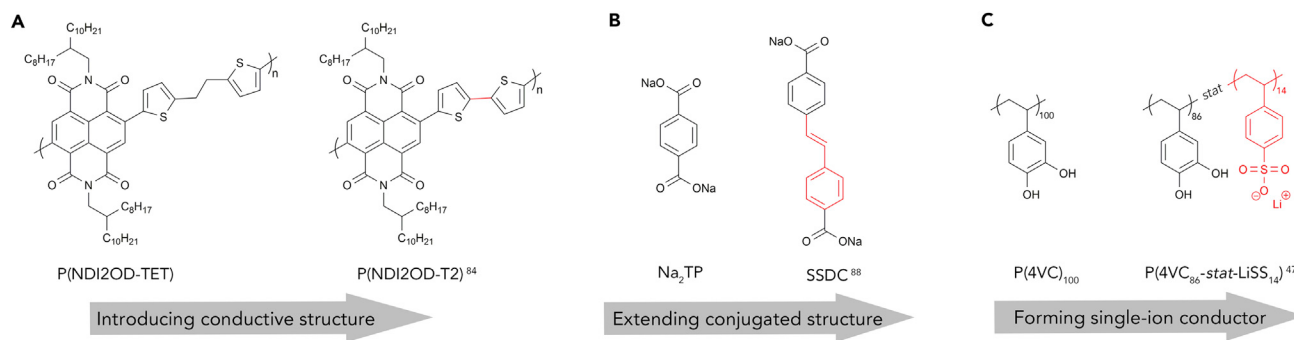


Figure 10. Improvement of Rate Performance by Molecular Engineering

(A) Structural formulas of P(NDI2OD-TET) and P(NDI2OD-T2).
(B) Structural formulas of Na₂TP and SSDC.
(C) Structural formulas of P(4VC)₁₀₀ and P(4VC₈₆-stat-LiSS₁₄).⁴⁷

the large molecular weight of the monomer. The design method can also be extended to develop other analogous π -conjugated redox polymers (e.g., the covalent grafting of TEMPO units on conductive PAn).⁸⁵ After introducing a conductive backbone, the sulfide-based polymer could still maintain 35% material activity at a high rate of 120 C (full charge and discharge in 30 s) in aqueous ZIBs.⁸⁶ Much better rate performance (1,600 C, 4.5 s per cycle) could be achieved by electropolymerizing 3,4-ethylenedioxy-thiophene within the pores of COFs because of the remarkably enhanced electronic conductivity.⁸⁷

Extending the π -conjugated structure of Na₂TP can form sodium 4,4'-stilbene-dicarboxylate (SSDC, Figure 10B). Compared with Na₂TP, SSDC exhibits enhanced charge transport, stable charged and discharged states, and improved intermolecular interactions, which are very beneficial for the sodiation and desodiation processes. Thus, SSDC still shows good capacity retention at a high rate of 10 A g⁻¹.⁸⁸ Nevertheless, as anode materials, the relatively low reversible capacity (<300 mAh g⁻¹) of SSDC could hardly satisfy the demand for practical applications. Further research should focus on designing highly conjugated molecules with more active sites per weight to achieve both high power density and high capacity.⁸⁹ Additionally, constructing single-ion conducting redox-active materials is also an effective way to enhance the rate capability. For example, after introducing -SO₃Li pendants to P(4VC)₁₀₀, Patil et al. obtained the single-ion conducting P(4VC₈₆-stat-LiSS₁₄) polymer (Figure 10C).⁴⁷ The reduced product can be stabilized and the ion transport from the active sites into the electrolyte can be improved by the -SO₃Li pendants, resulting in high capacity of 96 mAh g⁻¹ even at an extremely high rate of 600 C (6 s for whole discharge). It is noteworthy that the mass loading of active materials is only 20 wt % in the electrode.

Electrode Design

In addition to the structure of organic molecules, their specific area and the addition of conductive substrates also have much influence on the rate performance. High specific area is helpful for sufficient electrolyte infiltration and fast electron and ion diffusion, resulting in high rate capability. For example, the pristine 2,6-diamino-anthraquinone-based COFs (DAAQ-COFs) suffer from sluggish diffusion resulting from the dense stacking of planar sheets (Figure 11A).⁹⁰ After ball milling, the dense COFs can be exfoliated into nanosheets with thickness of approximately 5 nm (Figure 11B). Compared with pristine materials, the exfoliated COFs exhibit

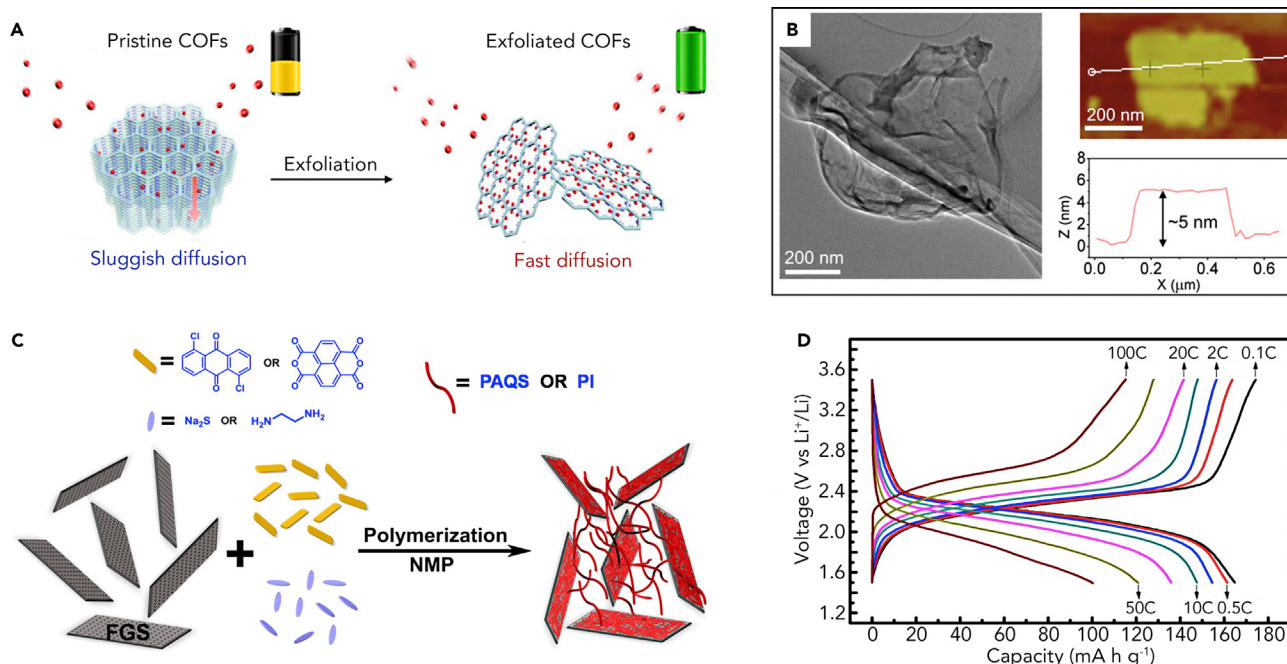


Figure 11. Improvement of Rate Performance by Electrode Design

(A and B) Schematic diagram for the exfoliation process of DAAQ-COFs (A) and transmission electron microscopy and atomic force microscopy images of the exfoliated COFs (B). Reprinted with permission from Wang et al.⁹⁰ Copyright 2017 American Chemical Society. (C and D) Schematic illustration for *in situ* polymerization of PAQS/graphene or polyimide/graphene composites (C) and charge-discharge profiles of the PAQS/graphene composite with 26 wt % graphene at different rates (D). Reprinted with permission from Song et al.⁹¹ Copyright 2012 American Chemical Society.

better capacity retention (50%) at 3 A g^{-1} . Another approach to increase the specific area of organic materials is by decreasing their particle size.

Combining organic materials with various highly conductive substrates such as graphene, CNTs, and carbon fibers can also enhance their rate capability in metal-ion batteries such as LIBs, ZIBs, and MIBs.^{17,24,64,89,91,92} The successful hybridization can be realized by simple mixing or *in situ* synthesis. For instance, Song et al. prepared the PAQS/graphene composites through *in situ* polymerization (Figure 11C).⁹¹ Compared with pure PAQS, the composite with 26 wt % graphene exhibit higher electronic conductivity (6.4×10^{-3} versus $1 \times 10^{-11} \text{ S cm}^{-1}$) and larger surface area (153 versus $30 \text{ cm}^2 \text{ g}^{-1}$). As a result, the composite can still maintain a discharge capacity of 100 mAh g^{-1} even at 100 C (16 s for whole discharge, Figure 11D). Analogously, the composite of $\text{Na}_2\text{C}_6\text{O}_6$ and graphene delivered a high capacity of 175 mAh g^{-1} even at 5 A g^{-1} in Mg-Li dual-ion batteries.⁶⁴ In general, to ensure good rate performance as well as high energy density, one should take into account the homogeneity of composites and the content and electronic conductivity of substrates.

In this section, the strategies toward enhancing the electrochemical performance (output voltage, capacity, cycling stability, and rate performance) of organic electrode materials in various metal-ion batteries have been overviewed. To help achieve more comprehensive understanding, we summarize the reported strategies in Figure 12. Generally, the strategies mainly include three aspects: molecular engineering, electrode design, and electrolyte and separator optimization. When specific strategies are to be adopted, the voltage, capacity, cycling stability, and rate

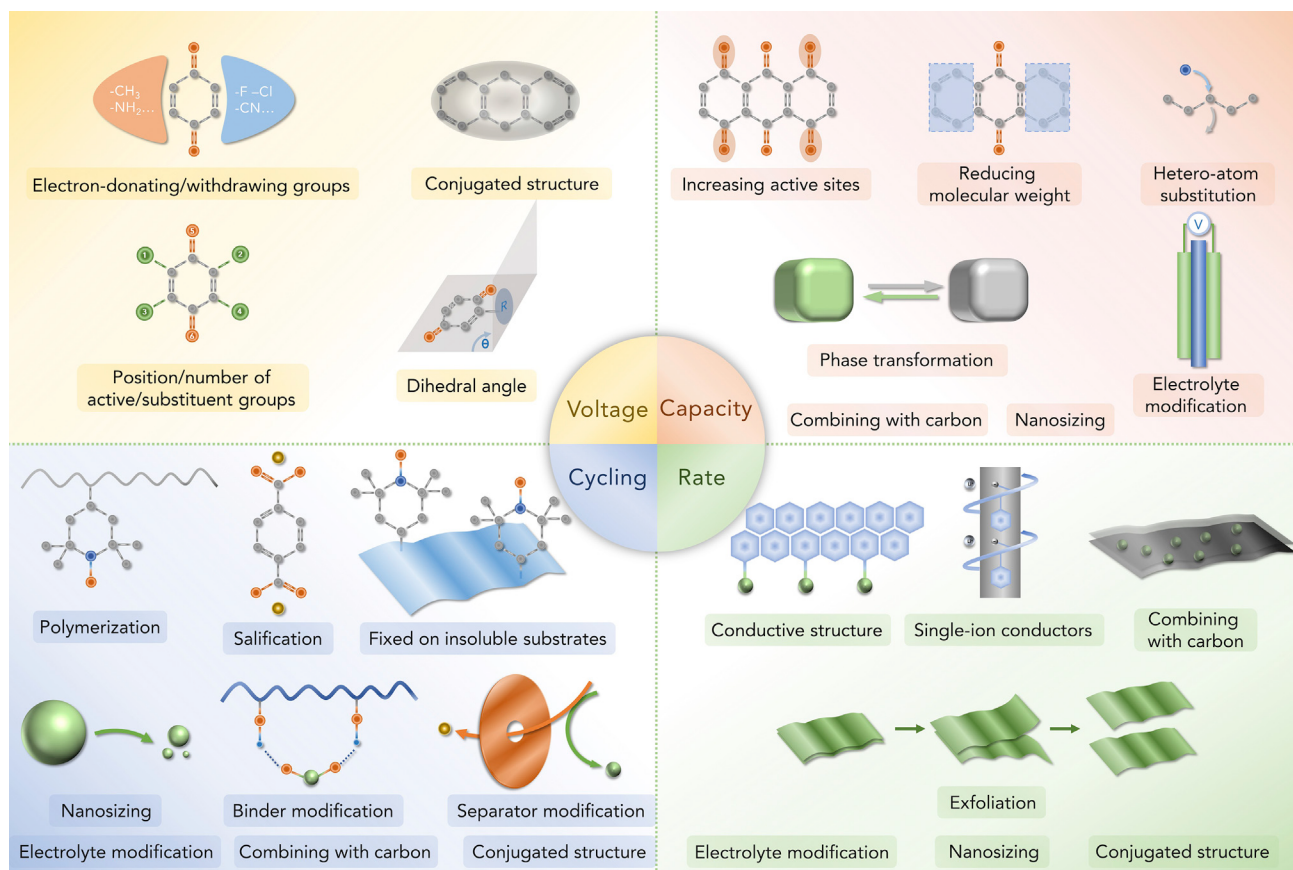


Figure 12. Summary of Design Strategies for Improving the Electrochemical Performance of Organic Electrode Materials in Metal-Ion Batteries

performance of organic materials should be considered simultaneously to achieve good comprehensive performance.

SUMMARY OF PERFORMANCE

Through various effective approaches, organic electrode materials can show enhanced electrochemical performance. The reported performance of different types of representative organic electrode materials in various metal-ion batteries are summarized in Table 3. The structural formulas of all organic molecules mentioned in Table 3 can be seen in Figure 13. The working principle and active sites of organic materials in different metal-ion batteries are similar. Thus, it is feasible to apply the same organic molecule in various metal-ion batteries. However, the electrochemical performance of organic electrode materials generally varies with the type of metal-ion batteries, which mainly results from the different ionic radius and valence of metal ions. The common rules can be summarized as follows:

- (1) The working voltage of organic molecules would be reduced when the ionic radius of metal ions increases.⁹⁴ Additionally, the voltage of the same molecule in multivalent-ion batteries is often higher than that in alkali metal-ion batteries.^{41,72,75,83} For example, the average discharge voltage of PAQS in metal-ion batteries follows the order MIBs > LIBs > SIBs > KIBs after eliminating the standard potential gap among the different metal anodes.^{13,56,58,99}

Table 3. Summary of the Electrochemical Performance of Representative Organic Electrode Materials in Various Metal-Ion Batteries

Battery Systems	Materials	Examples	Voltage (V)	Capacity ^a (mAh g ⁻¹)	Cycling Life (No. of Cycles)	Rate Capability (mAh g ⁻¹)	Active Materials Ratio ^b
Non-aqueous LIBs	conductive polymers	PPy ⁹³	3.0	140	100	110 (0.4 A g ⁻¹)	80%
	organosulfur compounds	DMTS ²⁰	2.0	658	50	317 (0.849 A g ⁻¹)	57%
		PDDTB ²²	2.2	378	20	—	40%
	organic radicals	PTMA ²⁴	3.5	222	20,000	80 (200 C)	10%
	carbonyl compounds	DTT ⁹²	1.5–3.0	292	200	220 (0.285 A g ⁻¹)	60%
		PBQS ⁹⁴	2.67	275	1,000	198 (5 A g ⁻¹)	60%
		DAAQ-COFs ⁹⁰	2.3	145	1,800	72.5 (3 A g ⁻¹)	60%
		Li ₄ DHTPA ⁷⁴	0.8	241	1,000	141 (2.41 A g ⁻¹)	60%
	imine compounds	3Q ⁸⁹	1.4–2.6	394	10,000	218 (8 A g ⁻¹)	30%
	cyano compounds	DCA ³²	1.3–2.0	200	30	—	50%
	azo compounds	ADALS ³³	1.45	190	5,000	105 (3.8 A g ⁻¹)	60%
	multiple carbon bonds	PPCQ ³⁶	0.2–1.0	1,678	1,000	269 (10 A g ⁻¹)	70%
Non-aqueous SIBs	conductive polymers	PANS ⁹⁵	2.4–3.6	133	200	76 (0.8 A g ⁻¹)	60%
	organic radicals	PTMA ⁷⁰	2.1, 3.36	222	100	190 (5 C)	63%
	carbonyl compounds	Na ₂ C ₆ O ₆ ⁹⁶	2.1	174	1,500	115 (5 A g ⁻¹)	70%
		PBQS ⁹⁴	2.08	268	100	140 (0.5 A g ⁻¹)	60%
		BP-COFs ⁵⁹	1.5–3.0	200	7,000	50 (5 A g ⁻¹)	70%
		SSDC ⁸⁸	0.5	220	400	72 (10 A g ⁻¹)	50%
	imine compounds	O ₂ -Na ²⁹	0.4–1.0	250	50	35 (1.29 A g ⁻¹)	80%
	azo compounds	ADASS ³⁴	1.25	170	2,000	71 (40 C)	60%
Non-aqueous KIBs	conductive polymers	PTPAn ⁹⁷	3.5–3.8	100	60	—	80%
	carbonyl compounds	PTCDA ⁹⁸	2.2–3.0	131	200	73 (0.5 A g ⁻¹)	70%
		PAQS ⁹⁹	1.6–2.2	190	200	—	70%
		K ₂ TP ⁶²	0.53	261	500	185 (1 A g ⁻¹)	60%
Non-aqueous MIBs	organosulfur compounds	CSM-PAn ²¹	1.4	117	22	—	77%
	carbonyl compounds	P14AQ ⁵⁸	1.1–1.8	133	1,000	48 (1.3 A g ⁻¹)	40%
Non-aqueous ZIBs	conductive polymers	PEDOT ¹⁷	1.2	42	100	27 (8 A g ⁻¹)	85%
Non-aqueous AlBs	conjugated polymers	PNPP ⁵²	1.7	150	1,000	79 (2 A g ⁻¹)	50%
Aqueous LIBs	carbonyl compounds	PNTCDA ^{100,c}	−0.7 to −0.4 (versus SCE)	157	50,000	25 (100 A g ⁻¹)	60%
Aqueous SIBs	carbonyl compounds	PNTCDA ^{100,c}	−0.8 to −0.4 (versus SCE)	140	50,000	28 (100 A g ⁻¹)	60%
Aqueous KIBs	carbonyl compounds	PAQS ^{54,c}	−0.6 (versus SHE)	200	1,350	162 (4.5 A g ⁻¹)	70%
Aqueous MIBs	carbonyl compounds	PPTO ^{54,c}	0.04 (versus SHE)	144	1,000	120 (0.28 A g ⁻¹)	60%
Aqueous ZIBs	conductive polymers	PANMTh ¹⁹	1.1	146	150	110 (5 mA cm ⁻²)	100%
	organosulfur compounds	PexTTF ⁸⁶	0.9–1.3	100	10,000	47 (15.96 A g ⁻¹)	50%
	organic radicals	PTVE ²³	1.73	131	500	131 (60 C)	100%
	carbonyl compounds	C4Q ⁸³	1.0	335	1,000	172 (1 A g ⁻¹)	60%

(Continued on next page)

Table 3. Continued

Battery Systems	Materials	Examples	Voltage (V)	Capacity ^a (mAh g ⁻¹)	Cycling Life (No. of Cycles)	Rate Capability (mAh g ⁻¹)	Active Materials Ratio ^b
Aqueous CIBs	carbonyl compounds	PNTCDA ⁵³	-0.5 (versus Ag/AgCl)	160	4,000	115 (3.7 A g ⁻¹)	60%

PPy, polypyrrole; DMTS, dimethyl trisulfide; PDDTB, poly(1,4-di(1,3-dithiolan-2-yl)benzene); PTMA, poly(2,2,6,6-tetramethyl-1-piperidinyloxy-4-yl methacrylate); DTT, dibenzo[b,j]thianthrene-5,7,12,14-tetraone; PBQS, poly(benzoquinonyl sulfide); DAAQ-COFs, 2,6-diamino-anthraquinone-based COFs; Li₄DHTPA, tetra-lithium salt of 2,5-dihydroxyterephthalic acid; 3Q, fused N-heteroaromatic triquinoxalinylene molecules; DCA, 9,10-dicyanoanthracene; ADALS, azobenzene-4,4'-dicarboxylic acid lithium salt; PPCQ, poly(1,4-dihydro-11H-pyrazino[2',3':3,4]cyclopenta[1,2-b]quinoxalin-11-one); PANS, poly(aniline-co-aminobenzenesulfonic sodium); Na₂C₆O₆, disodium rhodizonate; BP-COFs, bipolar porous COFs; SSDC, sodium 4,4'-stilbene-dicarboxylate; O2-Na, -COONa-based oligomeric Schiff base; ADASS, azobenzene-4,4'-dicarboxylic acid sodium salt; PTPAn, polytriphenylamine; PTCDA, 3,4,9,10-perylenetetracarboxylic dianhydride; PAQS, poly(anthraquinonyl sulfide); K₂TP, dipotassium terephthalate; CSM-PAn, conductive sulfur-containing material-polyaniline; P14AQ, 1,4-polyantraquinone; PEDOT, poly(3,4-ethylenedioxythiophene); PNPP, poly(nitropyrene-co-pyrene); PNTCDA, poly(1,4,5,8-naphthalenetetracarboxylic dianhydride); PPTO, poly(pyrene-4,5,9,10-tetraone) derivative; PANMTh, poly(aniline-co-N-methylthionine); PexTTF, 9,10-di(1,3-dithiol-2-ylidene)-9,10-dihydroanthracene-based polymer; PTVE, poly(2,2,6,6-tetramethylpiperidinyloxy-4-yl vinyl ether); C4Q, calix[4]quinone; SCE, saturated calomel electrode; SHE, standard hydrogen electrode.

^aThe capacity refers to the highest reversible discharge capacity.

^bThe active materials ratio means the mass fraction of organic active materials in working electrodes.

^cThe corresponding cathodes for PNTCDA, PAQS, and PPTO are I⁻, Ni(OH)₂, and Mg_xCuHCF, respectively, and the capacities are based on the mass of organic anodes in full batteries.

- (2) The capacity (utilization of active sites) is related to the valence of metal ions and steric hindrance. For instance, the carbonyl utilization of P14AQ and C4Q in LIBs could achieve 100%, whereas the utilization decreases in non-aqueous Mg-P14AQ (50%) and aqueous Zn-C4Q (75%) batteries.^{56,58,75,83}
- (3) The volume change of organic materials would be more serious after combining with larger metal ions, leading to poor cycling stability. For example, compared with LIBs, the capacity retention of pteridine derivatives in SIBs is only 50% after 20 cycles.³⁰
- (4) The rate performance of organic electrode materials can be affected by the migration and desolvation of metal ions. For example, the rate capability of poly(1,4,5,8-naphthalenetetracarboxylic dianhydride) in aqueous CIBs is better than that in aqueous MIBs because of the smaller ionic radius and more facile desolvation of hydrated Ca²⁺ ions.⁵³

CONCLUSIONS AND PERSPECTIVES

In summary, this review provides an overview of different types of organic electrode materials and effective strategies to enhance their electrochemical performance (output voltage, capacity, cycling stability, and rate performance) in various metal-ion batteries (LIBs, SIBs, KIBs, MIBs, ZIBs, AlBs, and CIBs). The common challenges of organic electrode materials are the high solubility in electrolyte, low intrinsic electronic conductivity, and large volume change. Polymerization, salification, hybridization with insoluble substrates, and optimization of electrolyte, binder, and separator are helpful in suppressing the dissolution problem. The electronic conductivity of organic materials can be enhanced by molecular engineering (conductive and conjugated structure and single-ion conductor) and combination with conductive substrates. Nanosizing and using a functional binder are proven as effective in mitigating the volume change and pulverization of active materials. Among all the strategies, developing all-solid-state electrolyte for organic batteries with nanosized active materials and highly conductive additives would be a good way to solve these challenges simultaneously.

Although great progress has been achieved, there is still a long way to go before realizing large-scale applications of organic electrode materials in metal-ion

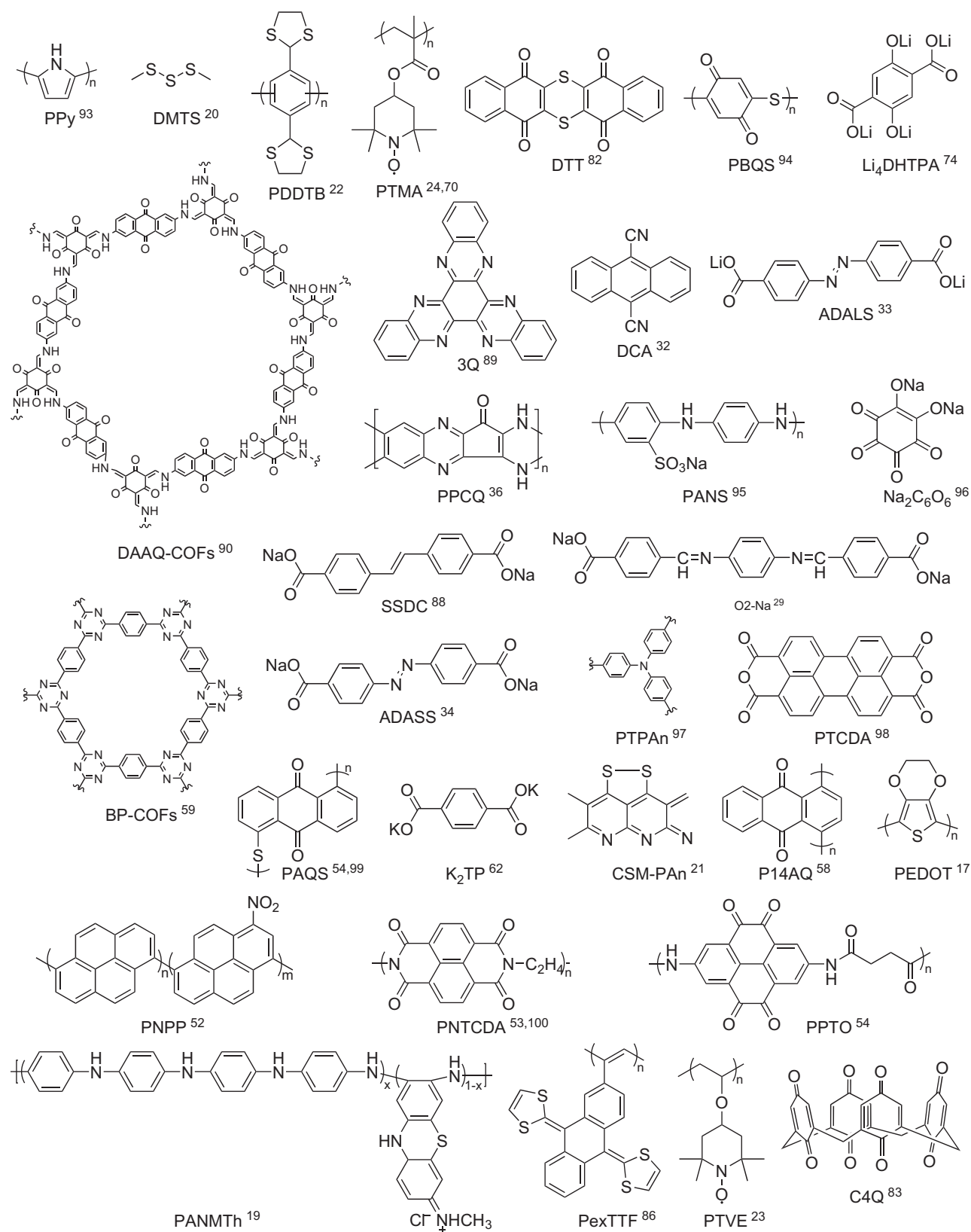


Figure 13. Structural Formulas of All Organic Molecules Mentioned in Table 3

batteries. This can be attributed to the following issues. (1) Because of their low electronic conductivity, large amounts of conductive carbons are added in the organic electrodes, leading to decreased energy density of the whole batteries. Moreover, the costs of some carbon materials with excellent conductivity, such as graphene and CNTs, are relatively high. (2) Organic materials consist of light elements (e.g., C, H, and O) and, as a result, their tap densities are generally low, which results in low volumetric energy density. (3) Since most n-type organic cathode materials do not contain metal ions initially, the anode sides need to provide metal ions, leading to limited available anode materials. Although p-type organic materials are not plagued by this problem, they have to consume large amounts of electrolyte. (4) Many organic materials, especially small molecules, show inferior thermal stability. In addition, the chemical stability of some organic molecules such as Li₄DHTPA (unstable in air) is not good. (5) Some high-performance organic materials such as carbonyl polymers can only be obtained by a complex fabrication process, which inevitably increases their production cost and limits their practical applications.

Considering the aforementioned problems, we strongly suggest that further research focus on the following aspects. First, elaborate molecular engineering could be developed to improve the intrinsic electronic conductivity and tap density of organic electrode materials and thus enhance the whole gravimetric and volumetric energy density of batteries. Second, high-performance solid-state electrolyte can be prepared for the assembly of metal-organic batteries because of their considerable energy density, high safety, and good cycling stability. Third, highly stable organic materials with metal ions initially are desired. Fourth and finally, for further applications, large-scale production of high-performance and stable organic materials via facile and scalable methods with low cost must be considered.

ACKNOWLEDGMENTS

This work was supported by the National Programs for Nano-Key Project (2017YFA0206700), the National Natural Science Foundation of China (21835004), and 111 Project from the Ministry of Education of China (B12015).

AUTHOR CONTRIBUTIONS

J.C. proposed the topic of the review. Y.L. conducted the literature search. Q.Z. organized the figures. L.L. designed the tables. J.C., Z.N., and Y.L. discussed, wrote, and revised the manuscript.

REFERENCES AND NOTES

1. Armand, M., and Tarascon, J.M. (2008). Building better batteries. *Nature* **451**, 652–657.
2. Zhang, K., Han, X., Hu, Z., Zhang, X., Tao, Z., and Chen, J. (2015). Nanostructured Mn-based oxides for electrochemical energy storage and conversion. *Chem. Soc. Rev.* **44**, 699–728.
3. Zeng, X., Zhan, C., Lu, J., and Amine, K. (2018). Stabilization of a high-capacity and high-power nickel-based cathode for Li-ion batteries. *Chem* **4**, 690–704.
4. Kim, J., Kim, J.H., and Ariga, K. (2017). Redox-active polymers for energy storage nanoarchitectonics. *Joule* **1**, 739–768.
5. Ding, Y., and Yu, G. (2017). Molecular engineering enables better organic flow batteries. *Chem* **3**, 917–919.
6. Williams, D.L., Byrne, J.J., and Driscoll, J.S. (1969). A high energy density lithium/dichloroisocyanuric acid battery system. *J. Electrochem. Soc.* **116**, 2–4.
7. Muench, S., Wild, A., Fribe, C., Häupler, B., Janoschka, T., and Schubert, U.S. (2016). Polymer-based organic batteries. *Chem. Rev.* **116**, 9438–9484.
8. Pickup, P.G., and Osteryoung, R.A. (1984). Electrochemical polymerization of pyrrole and electrochemistry of polypyrrole films in ambient temperature molten salts. *J. Am. Chem. Soc.* **106**, 2294–2299.
9. Visco, S.J., and DeJonghe, L.C. (1988). Ionic conductivity of organosulfur melts for advanced storage electrodes. *J. Electrochem. Soc.* **135**, 2905–2909.
10. Nakahara, K., Iwasa, S., Satoh, M., Morioka, Y., Iriyama, J., Suguro, M., and Hasegawa, E. (2002). Rechargeable batteries with organic radical cathodes. *Chem. Phys. Lett.* **359**, 351–354.
11. Wu, Y., Zeng, R., Nan, J., Shu, D., Qiu, Y., and Chou, S.-L. (2017). Quinone electrode materials for rechargeable lithium/sodium ion batteries. *Adv. Energy Mater.* **7**, 1700278.

12. Lee, S., Kwon, G., Ku, K., Yoon, K., Jung, S.-K., Lim, H.-D., and Kang, K. (2018). Recent progress in organic electrodes for Li and Na rechargeable batteries. *Adv. Mater.* 30, 1704682.
13. Zhao, Q., Lu, Y., and Chen, J. (2017). Advanced organic electrode materials for rechargeable sodium-ion batteries. *Adv. Energy Mater.* 7, 1601792.
14. Schon, T.B., McAllister, B.T., Li, P.-F., and Seferos, D.S. (2016). The rise of organic electrode materials for energy storage. *Chem. Soc. Rev.* 45, 6345–6404.
15. Xu, Y., Zhou, M., and Lei, Y. (2018). Organic materials for rechargeable sodium-ion batteries. *Mater. Today* 21, 60–78.
16. Zhu, L.M., Lei, A.W., Cao, Y.L., Ai, X.P., and Yang, H.X. (2013). An all-organic rechargeable battery using bipolar poly(etherphenylene) as a redox-active cathode and anode. *Chem. Commun. (Camb.)* 49, 567–569.
17. Simons, T.J., Salsamendi, M., Howlett, P.C., Forsyth, M., MacFarlane, D.R., and Pozo-Gonzalo, C. (2015). Rechargeable Zn/PEDOT battery with an imidazolium-based ionic liquid as the electrolyte. *ChemElectroChem* 2, 2071–2078.
18. Hudak, N.S. (2014). Chloroaluminate-doped conducting polymers as positive electrodes in rechargeable aluminum batteries. *J. Phys. Chem. C* 118, 5203–5215.
19. Chen, C., Hong, X., Chen, A., Xu, T., Lu, L., Lin, S., and Gao, Y. (2016). Electrochemical properties of poly(aniline-co-N-methylthionine) for zinc-conducting polymer rechargeable batteries. *Electrochim. Acta* 190, 240–247.
20. Wu, M., Cui, Y., Bhargav, A., Losovjy, Y., Siegel, A., Agarwal, M., Ma, Y., and Fu, Y. (2016). Organotrisulfide: a high capacity cathode material for rechargeable lithium batteries. *Angew. Chem. Int. Ed.* 55, 10027–10031.
21. Nuli, Y., Guo, Z., Liu, H., and Yang, J. (2007). A new class of cathode materials for rechargeable magnesium batteries: organosulfur compounds based on sulfur-sulfur bonds. *Electrochem. Commun.* 9, 1913–1917.
22. Zhang, J.Y., Kong, L.B., Zhan, L.Z., Tang, J., Zhan, H., Zhou, Y.H., and Zhan, C.M. (2007). Sulfides organic polymer: novel cathode active material for rechargeable lithium batteries. *J. Power Sources* 168, 278–281.
23. Koshika, K., Sano, N., Oyaizu, K., and Nishide, H. (2009). An aqueous, electrolyte-type, rechargeable device utilizing a hydrophilic radical polymer-cathode. *Macromol. Chem. Phys.* 210, 1989–1995.
24. Guo, W., Yin, Y.-X., Xin, S., Guo, Y.-G., and Wan, L.-J. (2012). Superior radical polymer cathode material with a two-electron process redox reaction promoted by graphene. *Energy Environ. Sci.* 5, 5221–5225.
25. Jähnert, T., Häpler, B., Janoschka, T., Hager, M.D., and Schubert, U.S. (2013). Synthesis and charge-discharge studies of poly(ethynylphenyl)galvinoxyles and their use in organic radical batteries with aqueous electrolytes. *Macromol. Chem. Phys.* 214, 2616–2623.
26. Jähnert, T., Hager, M.D., and Schubert, U.S. (2016). Assorted phenoxyl-radical polymers and their application in lithium-organic batteries. *Macromol. Rapid Commun.* 37, 725–730.
27. Reddy, T.B. (2011). *Linden's Handbook of Batteries*, Fourth Edition (McGraw-Hill Education).
28. Rodríguez-Pérez, I.A., Yuan, Y., Bommier, C., Wang, X., Ma, L., Leonard, D.P., Lerner, M.M., Carter, R.G., Wu, T., Greaney, P.A., et al. (2017). Mg-ion battery electrode: an organic solid's herringbone structure squeezed upon Mg-ion insertion. *J. Am. Chem. Soc.* 139, 13031–13037.
29. López-Herraiz, M., Castillo-Martínez, E., Carretero-González, J., Carrasco, J., Rojo, T., and Armand, M. (2015). Oligomeric-Schiff bases as negative electrodes for sodium ion batteries: unveiling the nature of their active redox centers. *Energy Environ. Sci.* 8, 3233–3241.
30. Hong, J., Lee, M., Lee, B., Seo, D.-H., Park, C.B., and Kang, K. (2014). Biologically inspired pteridine redox centres for rechargeable batteries. *Nat. Commun.* 5, 5335.
31. Tian, B., Ding, Z., Ning, G.-H., Tang, W., Peng, C., Liu, B., Su, J., Su, C., and Loh, K.P. (2017). Amino group enhanced phenazine derivatives as electrode materials for lithium storage. *Chem. Commun. (Camb.)* 53, 2914–2917.
32. Deng, Q., He, S.-J., Pei, J., Fan, C., Li, C., Cao, B., Lu, Z.-H., and Li, J. (2017). Exploitation of redox-active 1,4-dicyanobenzene and 9,10-dicyanoanthracene as the organic electrode materials in rechargeable lithium battery. *Electrochem. Commun.* 75, 29–32.
33. Luo, C., Borodin, O., Ji, X., Hou, S., Gaskell, K.J., Fan, X., Chen, J., Deng, T., Wang, R., Jiang, J., et al. (2018). Azo compounds as a family of organic electrode materials for alkali-ion batteries. *Proc. Natl. Acad. Sci. USA* 115, 2004–2009.
34. Luo, C., Xu, G.-L., Ji, X., Hou, S., Chen, L., Wang, F., Jiang, J., Chen, Z., Ren, Y., Amine, K., et al. (2018). Reversible redox chemistry of azo compounds for sodium-ion batteries. *Angew. Chem. Int. Ed.* 57, 2879–2883.
35. Renault, S., Oltean, V.A., Araujo, C.M., Grigoriev, A., Edström, K., and Brandell, D. (2016). Superlithiation of organic electrode materials: the case of dilithium benzenedipropionate. *Chem. Mater.* 28, 1920–1926.
36. Xie, J., Rui, X., Gu, P., Wu, J., Xu, Z.J., Yan, Q., and Zhang, Q. (2016). Novel conjugated ladder-structured oligomer anode with high lithium storage and long cycling capability. *ACS Appl. Mater. Interfaces* 8, 16932–16938.
37. Lu, Y., Lu, Y., Niu, Z., and Chen, J. (2018). Graphene-based nanomaterials for sodium-ion batteries. *Adv. Energy Mater.* 8, 1702469.
38. Liang, Y., Zhang, P., Yang, S., Tao, Z., and Chen, J. (2013). Fused heteroaromatic organic compounds for high-power electrodes of rechargeable lithium batteries. *Adv. Energy Mater.* 3, 600–605.
39. Armand, M., Gruegeon, S., Vezin, H., Laruelle, S., Ribière, P., Poizot, P., and Tarascon, J.M. (2009). Conjugated dicarboxylate anodes for Li-ion batteries. *Nat. Mater.* 8, 120–125.
40. Yokoi, T., Matsubara, H., and Satoh, M. (2014). Rechargeable organic lithium-ion batteries using electron-deficient benzooquinones as positive-electrode materials with high discharge voltages. *J. Mater. Chem. A* 2, 19347–19354.
41. Kim, H., Kwon, J.E., Lee, B., Hong, J., Lee, M., Park, S.Y., and Kang, K. (2015). High energy organic cathode for sodium rechargeable batteries. *Chem. Mater.* 27, 7258–7264.
42. Lu, Y., Zhao, Q., Miao, L.C., Tao, Z.L., Niu, Z.Q., and Chen, J. (2017). Flexible and free-standing organic/carbon nanotubes hybrid films as cathode for rechargeable lithium-ion batteries. *J. Phys. Chem. C* 121, 14498–14506.
43. Lee, J., Kim, H., and Park, M.J. (2016). Long-life, high-rate lithium-organic batteries based on naphthoquinone derivatives. *Chem. Mater.* 28, 2408–2416.
44. Xiang, J., Chang, C., Li, M., Wu, S., Yuan, L., and Sun, J. (2008). A novel coordination polymer as positive electrode material for lithium ion battery. *Cryst. Growth Des.* 8, 280–282.
45. Zhu, Z., Li, H., Liang, J., Tao, Z., and Chen, J. (2015). The disodium salt of 2,5-dihydroxy-1,4-benzoquinone as anode material for rechargeable sodium ion batteries. *Chem. Commun. (Camb.)* 51, 1446–1448.
46. Gotti, S., Barrès, A.-L., Dolhem, F., and Poizot, P. (2014). Voltage gain in lithiated enolate-based organic cathode materials by isomeric effect. *ACS Appl. Mater. Interfaces* 6, 10870–10876.
47. Patil, N., Aqil, A., Ouhib, F., Admassie, S., Inganás, O., Jérôme, C., and Detrembleur, C. (2017). Bioinspired redox-active catechol-bearing polymers as ultrarobust organic cathodes for lithium storage. *Adv. Mater.* 29, 1703373.
48. Wu, D., Xie, Z., Zhou, Z., Shen, P., and Chen, Z. (2015). Designing high-voltage carbonyl-containing polycyclic aromatic hydrocarbon cathode materials for Li-ion batteries guided by Clar's theory. *J. Mater. Chem. A* 3, 19137–19143.
49. Banda, H., Damien, D., Nagarajan, K., Raj, A., Hariharan, M., and Shaijumon, M.M. (2017). Twisted perylene diimides with tunable redox properties for organic sodium-ion batteries. *Adv. Energy Mater.* 7, 1701316.
50. Lee, M., Hong, J., Lopez, J., Sun, Y., Feng, D., Lim, K., Chueh, W.C., Toney, M.F., Cui, Y., and Bao, Z. (2017). High-performance sodium-organic battery by realizing four-sodium storage in disodium rhodizonate. *Nat. Energy* 2, 861–868.
51. Zhao, H., Wang, J., Zheng, Y., Li, J., Han, X., He, G., and Du, Y. (2017). Organic thiocarboxylate electrodes for a room-temperature sodium-ion battery delivering an ultrahigh capacity. *Angew. Chem. Int. Ed.* 56, 15334–15338.

52. Walter, M., Kravchyk, K.V., Böfer, C., Widmer, R., and Kovalenko, M.V. (2018). Polypyrenes as high-performance cathode materials for aluminum batteries. *Adv. Mater.* 30, 1705644.
53. Gheytani, S., Liang, Y., Wu, F., Jing, Y., Dong, H., Rao, K.K., Chi, X., Fang, F., and Yao, Y. (2017). An aqueous ca-ion battery. *Adv. Sci.* 4, 1700465.
54. Liang, Y., Jing, Y., Gheytani, S., Lee, K.-Y., Liu, P., Facchetti, A., and Yao, Y. (2017). Universal quinone electrodes for long cycle life aqueous rechargeable batteries. *Nat. Mater.* 16, 841–848.
55. Zhang, K., Hu, Y., Wang, L., Fan, J., Monteiro, M.J., and Jia, Z. (2017). The impact of the molecular weight on the electrochemical properties of poly(TEMPO methacrylate). *Polym. Chem.* 8, 1815–1823.
56. Song, Z., Qian, Y., Gordin, M.L., Tang, D., Xu, T., Otani, M., Zhan, H., Zhou, H., and Wang, D. (2015). Polyanthraquinone as a reliable organic electrode for stable and fast lithium storage. *Angew. Chem. Int. Ed.* 54, 13947–13951.
57. Bitenc, J., Pirnat, K., Bančić, T., Gaberšček, M., Genorio, B., Randon-Vitanova, A., and Dominko, R. (2015). Anthraquinone-based polymer as cathode in rechargeable magnesium batteries. *ChemSusChem* 8, 4128–4132.
58. Pan, B., Huang, J., Feng, Z., Zeng, L., He, M., Zhang, L., Vaughey, J.T., Bedzyk, M.J., Fenter, P., Zhang, Z., et al. (2016). Polyanthraquinone-based organic cathode for high-performance rechargeable magnesium-ion batteries. *Adv. Energy Mater.* 6, 1600140.
59. Sakaushi, K., Hosono, E., Nickerl, G., Gemming, T., Zhou, H., Kaskel, S., and Eckert, J. (2013). Aromatic porous-honeycomb electrodes for a sodium-organic energy storage device. *Nat. Commun.* 4, 1485.
60. Lin, Z.-Q., Xie, J., Zhang, B.-W., Li, J.-W., Weng, J., Song, R.-B., Huang, X., Zhang, H., Li, H., Liu, Y., et al. (2017). Solution-processed nitrogen-rich graphene-like holey conjugated polymer for efficient lithium ion storage. *Nano Energy* 41, 117–127.
61. DeBlase, C.R., Hernández-Burgos, K., Rotter, J.M., Fortman, D.J., Abreu Ddos, S., Timm, R.A., Diógenes, I.C.N., Kubota, L.T., Abruna, H.D., and Dichtel, W.R. (2015). Cation-dependent stabilization of electrogenerated naphthalene diimide dianions in porous polymer thin films and their application to electrical energy storage. *Angew. Chem. Int. Ed.* 54, 13225–13229.
62. Lei, K., Li, F., Mu, C., Wang, J., Zhao, Q., Chen, C., and Chen, J. (2017). High K-storage performance based on the synergy of dipotassium terephthalate and ether-based electrolytes. *Energy Environ. Sci.* 10, 552–557.
63. Park, Y., Shin, D.-S., Woo, S.H., Choi, N.S., Shin, K.H., Oh, S.M., Lee, K.T., and Hong, S.Y. (2012). Sodium terephthalate as an organic anode material for sodium ion batteries. *Adv. Mater.* 24, 3562–3567.
64. Tian, J., Cao, D., Zhou, X., Hu, J., Huang, M., and Li, C. (2018). High-capacity Mg-organic batteries based on nanostructured rhodizionate salts activated by Mg-Li dual-salt electrolyte. *ACS Nano* 12, 3424–3435.
65. Wang, S., Wang, L., Zhang, K., Zhu, Z., Tao, Z., and Chen, J. (2013). Organic $\text{Li}_4\text{C}_8\text{H}_2\text{O}_6$ nanosheets for lithium-ion batteries. *Nano Lett.* 13, 4404–4409.
66. Wang, S., Wang, L., Zhu, Z., Hu, Z., Zhao, Q., and Chen, J. (2014). All organic sodium-ion batteries with $\text{Na}_4\text{C}_8\text{H}_2\text{O}_6$. *Angew. Chem. Int. Ed.* 53, 5892–5896.
67. Wan, W., Lee, H., Yu, X., Wang, C., Nam, K.-W., Yang, X.-Q., and Zhou, H. (2014). Tuning the electrochemical performances of anthraquinone organic cathode materials for Li-ion batteries through the sulfonic sodium functional group. *RSC Adv.* 4, 19878–19882.
68. Lee, M., Hong, J., Kim, H., Lim, H.-D., Cho, S.B., Kang, K., and Park, C.B. (2014). Organic nanohybrids for fast and sustainable energy storage. *Adv. Mater.* 26, 2558–2565.
69. Wang, H., Hu, P., Yang, J., Gong, G., Guo, L., and Chen, X. (2015). Renewable-Juglone-based high-performance sodium-ion batteries. *Adv. Mater.* 27, 2348–2354.
70. Kim, J.-K., Kim, Y., Park, S., Ko, H., and Kim, Y. (2016). Encapsulation of organic active materials in carbon nanotubes for application to high-electrochemical-performance sodium batteries. *Energy Environ. Sci.* 9, 1264–1269.
71. Guo, C., Zhang, K., Zhao, Q., Pei, L., and Chen, J. (2015). High-performance sodium batteries with the 9,10-anthraquinone/CMK-3 cathode and an ether-based electrolyte. *Chem. Commun. (Camb.)* 51, 10244–10247.
72. Kundu, D., Oberholzer, P., Glaros, C., Bouzid, A., Tervoort, E., Pasquarello, A., and Niederberger, M. (2018). Organic cathode for aqueous Zn-ion batteries: taming a unique phase evolution toward stable electrochemical cycling. *Chem. Mater.* 30, 3874–3881.
73. Lin, H.-C., Li, C.-C., and Lee, J.-T. (2011). Nitroxide polymer brushes grafted onto silica nanoparticles as cathodes for organic radical batteries. *J. Power Sources* 196, 8098–8103.
74. Zhao, Q., Wang, J., Chen, C., Ma, T., and Chen, J. (2017). Nanostructured organic electrode materials grown on graphene with covalent-bond interaction for high-rate and ultra-long-life lithium-ion batteries. *Nano Res.* 10, 4245–4255.
75. Huang, W., Zhu, Z., Wang, L., Wang, S., Li, H., Tao, Z., Shi, J., Guan, L., and Chen, J. (2013). Quasi-solid-state rechargeable lithium-ion batteries with a calix[4]quinone cathode and gel polymer electrolyte. *Angew. Chem. Int. Ed.* 52, 9162–9166.
76. Chi, X., Liang, Y., Hao, F., Zhang, Y., Whiteley, J., Dong, H., Hu, P., Lee, S., and Yao, Y. (2018). Tailored organic electrode material compatible with sulfide electrolyte for stable all-solid-state sodium batteries. *Angew. Chem. Int. Ed.* 57, 2630–2634.
77. Wu, S., Wang, W., Li, M., Cao, L., Lyu, F., Yang, M., Wang, Z., Shi, Y., Nan, B., Yu, S., et al. (2016). Highly durable organic electrode for sodium-ion batteries via a stabilized α -C radical intermediate. *Nat. Commun.* 7, 13318.
78. Kolek, M., Otteny, F., Schmidt, P., Mück-Lichtenfeld, C., Einholz, C., Becking, J., Schleicher, E., Winter, M., Bieker, P., and Esser, B. (2017). Ultra-high cycling stability of poly(vinylphenothiazine) as a battery cathode material resulting from π - π interactions. *Energy Environ. Sci.* 10, 2334–2341.
79. Wang, Y., Ding, Y., Pan, L., Shi, Y., Yue, Z., Shi, Y., and Yu, G. (2016). Understanding the size-dependent sodium storage properties of $\text{Na}_2\text{C}_6\text{O}_6$ -based organic electrodes for sodium-ion batteries. *Nano Lett.* 16, 3329–3334.
80. Luo, C., Fan, X., Ma, Z., Gao, T., and Wang, C. (2017). Self-healing chemistry between organic material and binder for stable sodium-ion batteries. *Chem* 3, 1050–1062.
81. Song, Z., Qian, Y., Otani, M., and Zhou, H. (2016). Stable Li-organic batteries with Nafion-based sandwich-type separators. *Adv. Energy Mater.* 6, 1501780.
82. Ma, T., Zhao, Q., Wang, J., Pan, Z., and Chen, J. (2016). A sulfur heterocyclic quinone cathode and a multifunctional binder for a high-performance rechargeable lithium-ion battery. *Angew. Chem. Int. Ed.* 55, 6428–6432.
83. Zhao, Q., Huang, W., Luo, Z., Liu, L., Lu, Y., Li, Y., Li, L., Hu, J., Ma, H., and Chen, J. (2018). High-capacity aqueous zinc batteries using sustainable quinone electrodes. *Sci. Adv.* 4, eaao1761.
84. Liang, Y., Chen, Z., Jing, Y., Rong, Y., Facchetti, A., and Yao, Y. (2015). Heavily n-dopable π -conjugated redox polymers with ultrafast energy storage capability. *J. Am. Chem. Soc.* 137, 4956–4959.
85. Oyaizu, K., Tatsuhira, H., and Nishide, H. (2015). Facile charge transport and storage by a TEMPO-populated redox mediating polymer integrated with polyaniline as electrical conducting path. *Polymer J.* 47, 212–219.
86. Häupler, B., Rössel, C., Schwenke, A.M., Winsberg, J., Schmidt, D., Wild, A., and Schubert, U.S. (2016). Aqueous zinc-organic polymer battery with a high rate performance and long lifetime. *NPG Asia Mater.* 8, e283.
87. Mulzer, C.R., Shen, L., Bisbey, R.P., McKone, J.R., Zhang, N., Abruna, H.D., and Dichtel, W.R. (2016). Superior charge storage and power density of a conducting polymer-modified covalent organic framework. *ACS Cent. Sci.* 2, 667–673.
88. Wang, C., Xu, Y., Fang, Y., Zhou, M., Liang, L., Singh, S., Zhao, H., Schober, A., and Lei, Y. (2015). Extended π -conjugated system for fast-charge and -discharge sodium-ion batteries. *J. Am. Chem. Soc.* 137, 3124–3130.
89. Peng, C., Ning, G.-H., Su, J., Zhong, G., Tang, W., Tian, B., Su, C., Yu, D., Zu, L., Yang, J., et al. (2017). Reversible multi-electron redox chemistry of π -conjugated N-containing heteroaromatic molecule-based organic cathodes. *Nat. Energy* 2, 17074.
90. Wang, S., Wang, Q., Shao, P., Han, Y., Gao, X., Ma, L., Yuan, S., Ma, X., Zhou, J., Feng, X., et al. (2017). Exfoliation of covalent

- organic frameworks into few-layer redox-active nanosheets as cathode materials for lithium-ion batteries. *J. Am. Chem. Soc.* 139, 4258–4261.
91. Song, Z., Xu, T., Gordin, M.L., Jiang, Y.-B., Bae, I.-T., Xiao, Q., Zhan, H., Liu, J., and Wang, D. (2012). Polymer-graphene nanocomposites as ultrafast-charge and -discharge cathodes for rechargeable lithium batteries. *Nano Lett.* 12, 2205–2211.
92. Amin, K., Meng, Q., Ahmad, A., Cheng, M., Zhang, M., Mao, L., Lu, K., and Wei, Z. (2018). A carbonyl compound-based flexible cathode with superior rate performance and cyclic stability for flexible lithium-ion batteries. *Adv. Mater.* 30, 1703868.
93. Zhou, M., Qian, J., Ai, X., and Yang, H. (2011). Redox-active $\text{Fe}(\text{CN})_6^{4-}$ -doped conducting polymers with greatly enhanced capacity as cathode materials for Li-ion batteries. *Adv. Mater.* 23, 4913–4917.
94. Song, Z., Qian, Y., Zhang, T., Otani, M., and Zhou, H. (2015). Poly(benzoquinonyl sulfide) as a high-energy organic cathode for rechargeable Li and Na batteries. *Adv. Sci. 2*, 1500124.
95. Zhou, M., Li, W., Gu, T., Wang, K., Cheng, S., and Jiang, K. (2015). A sulfonated polyaniline with high density and high rate Na-storage performances as a flexible organic cathode for sodium ion batteries. *Chem. Commun. (Camb.)* 51, 14354–14356.
96. Wang, C., Fang, Y., Xu, Y., Liang, L., Zhou, M., Zhao, H., and Lei, Y. (2016). Manipulation of disodium rhodizonate: factors for fast-charge and fast-discharge sodium-ion batteries with long-term cyclability. *Adv. Funct. Mater.* 26, 1777–1786.
97. Fan, L., Liu, Q., Xu, Z., and Lu, B. (2017). An organic cathode for potassium dual-ion full battery. *ACS Energy Lett.* 2, 1614–1620.
98. Chen, Y., Luo, W., Carter, M., Zhou, L., Dai, J., Fu, K., Lacey, S., Li, T., Wan, J., Han, X., et al. (2015). Organic electrode for non-aqueous potassium-ion batteries. *Nano Energy* 18, 205–211.
99. Jian, Z., Liang, Y., Rodríguez-Pérez, I.A., Yao, Y., and Ji, X. (2016). Poly(anthraquinonyl sulfide) cathode for potassium-ion batteries. *Electrochim. Commun.* 71, 5–8.
100. Dong, X., Chen, L., Liu, J., Haller, S., Wang, Y., and Xia, Y. (2016). Environmentally-friendly aqueous Li (or Na)-ion battery with fast electrode kinetics and super-long life. *Sci. Adv.* 2, e1501038.